NORWEGIAN JOURNAL OF GEOLOGY
https://dx.doi.org/10.17850/njg104-1-3

GEOLOGICAL SOCIETY OF NORWAY

Episodic anorthosite-mangerite-charnockite-granite (AMCG) plutonism in Rogaland, South Norway: the 1.24 Ga Gloppurdi and Botnavatn fayalite-bearing charnockitic intrusions

Keywords:
- *AMCG plutonism*
- *Anorthosite*
- *Zr-rich jotunite*
- *C*harnockite
- *S*hear zone
- *Fayalite-bearing quartz mangerite*

Jean-Clair Duchesne[1], Bernard Bingen[2], Edith Wilmart[1,3], Marie Graulich[1,4], Magdalena H. Huyskens[2]

[1]*Department of Geology, University of Liège, 4000 Liège, Belgium*
[2]*Geological Survey of Norway, 7491 Trondheim, Norway*
[3]*Present address: CNRS, avenue de la Terrasse 1, Bâtiment 31, 91198 Gif-sur-Yvette, France*
[4]*Present address: Rue du Voisin 80, 5060 Auvelais, Belgium*

E-mail corresponding author (Jean-Clair Duchesne): jc.duchesne@uliege.be

Electronic supplement 1:
Table S1. Sampling and petrography of the Gloppurdi and Botnavatn intrusions.

Electronic supplement 2:
Table S2. Whole-rock geochemical and normative compositions of samples from the Gloppurdi and Botnavatn intrusions.

Electronic supplement 3:
Table S3. Summary of analytical conditions for zircon U–Pb analyses by LA–ICP–MS and values for secondary standards.

Electronic supplement 4:
Table S4. Zircon U–Pb geochronological data for the Gloppurdi and Botnavatn intrusions.

Received:
19. June 2023

Accepted:
25. April 2024

Published online:
X.X. October 2024

This study addresses the episodic nature of Proterozoic anorthosite-mangerite-charnockite-granite (AMCG) plutonism in the Sveconorwegian orogen in South Norway. Field, petrographic, major and trace element data are reported on the Gloppurdi and Botnavatn intrusions, dated together at 1236 ± 8 Ma (U–Pb zircon, 3 samples). These two small, foliated plutons are dominated by fayalite-bearing charnockitoid (mangerite, quartz mangerite and charnockite), and were emplaced some 300 Myr before the large and nearby 932–915 Ma AMCG complex, known as the Rogaland Anorthosite Province (RAP). The characteristic fayalite-bearing charnockitoid is ferroan (Mg# < 0.1), alkalic and metaluminous. The large variation in composition (60 < SiO_2 < 75 wt.%) is explained by variable clustering of mafic minerals. The rocks display major element compositions similar to the fayalite-bearing quartz mangerite of the Bjerkreim–Sokndal (BKSK) layered intrusion in the RAP. Zr, Th, U and REE compositions link the group to Zr-rich jotunite, a typical kindred rock type of AMCG plutonism. This suggests the occurrence of concealed magma chambers at 1.24 Ga in which anorthosite and related rocks possibly developed. Episodic AMCG plutonism thus possibly punctuated the regional evolution between 1.24 and 0.85 Ga.

Highlights

- The Gloppurdi and Botnavatn intrusions, Sveconorwegian orogen, Rogaland, South Norway.
- Fayalite-bearing mangerite, quartz mangerite and charnockite dominate.
- Zircon U–Pb data yield intrusion age at 1236 ± 8 Ma and metamorphism at 1013 ± 12 Ma.
- Fayalite-bearing charnockitoid is ferroan (Mg# < 0.1), alkalic, metaluminous and Zr-rich.
- Fayalite-bearing charnockitoid links Gloppurdi and Botnavatn to AMCG plutonism.
- Fayalite-bearing charnockitoid compares to Zr-rich jotunite in AMCG plutonism.
- Concealed AMCG magmatic system at c. 1240 Ma is possible.

Duchesne, J.C., Bingen, B., Wilmart, E., Graulich, M. & Huyskens, M.H. 2024: Episodic anorthosite-mangerite-charnockite-granite (AMCG) plutonism in Rogaland, South Norway: the 1.24 Ga Gloppurdi and Botnavatn fayalite-bearing charnockitic intrusions. *Norwegian Journal of Geology 104*, 202403.
https://dx.doi.org/10.17850/njg104-1-3

Introduction

The anorthosite-mangerite-charnockite-granite (AMCG) plutonism, also known as massif-type anorthosite plutonism, is specifically Proterozoic in age (Ashwal & Bybee, 2017). It associates anorthosites with (coeval) felsic rocks (Emslie, 1978; Emslie et al., 1994). The relationships between the felsic rocks and the anorthosites and related mafic rocks are still debated. One model considers that the felsic rocks are coeval but not comagmatic with anorthosites (references in McLelland et al., 2004). They result from partial melting of crustal rocks, the necessary heat being produced by the anorthosite plutonism. A second model links the felsic rocks to a magma of jotunitic composition, parental to andesine anorthosite (Demaiffe & Hertogen, 1981; Duchesne & Hertogen, 1988; Robins et al., 1997; Bolle et al., 2003), through fractional crystallization and crustal contamination (e.g., Duchesne & Wilmart, 1997; Vander Auwera et al., 1998; Bolle et al., 2003). Both models are not exclusive and give rise to characteristic rock types. The felsic rocks are charnockitic in that they contain orthopyroxene or fayalite + quartz and, frequently, mesoperthitic K-feldspar (Streckeisen, 1973). Chemically, they are ferroan and alkalic following Frost et al. (2001), potassic (very high-K, Peccerillo & Taylor, 1976), rich in LILE, REE, HFSE and, importantly, anhydrous. The fO_2 is close to FMQ conditions.

Another debate concerns the duration and periodicity of AMCG plutonism. Collection of reliable geochronological data over the last decades shows a significant dispersion of dates for a number of anorthosite provinces. It implies that anorthosite provinces commonly comprise distinct suites, each of them long-lived (Higgins & van Breemen, 1996; Scoates & Chamberlain, 1997; Hamilton et al., 1998; Connelly & Ryan, 1999; Myers et al., 2008; Raith et al., 2014; Bybee et al., 2019; Fourny et al., 2019). Proterozoic anorthosite plutons are characterized by the presence of high-alumina orthopyroxene megacrysts (HAOMs) (Emslie, 1975). For several anorthosite provinces, Sm–Nd data collected on HAOMs yield isochron ages some 80 to 120 Myr older than the intrusion age of their host anorthosite (Bybee et al., 2014). This feature is further evidence for a protracted or episodic nature of AMCG magmatism. Repetition of AMCG plutonism over time intervals of 100 Myr or more in the same area led some authors to propose a relation between AMCG plutonism and persistent lithospheric-scale shear zones, weakness zones, lineaments, suture zones or extension zones (Higgins & van Breemen, 1996; Scoates & Chamberlain, 1997; Duchesne et al., 1999; Krause et al., 2001; Myers et al., 2008). Reactivation of these structures above a mantle with a positive temperature anomaly may have facilitated reactivation of similar magma sources and channelled emplacement of anorthosite plutons to middle crustal levels.

The Rogaland Anorthosite Province (RAP) in South Norway (Fig. 1) is a typical example of Proterozoic AMCG plutonism (Duchesne et al., 1985b; Wilson et al., 1996; Marker et al., 2003; Vander Auwera et al., 2011). It formed at the end of the Sveconorwegian orogenic cycle at c. 930 Ma (Schärer et al., 1996; Vander Auwera et al., 2011) and carries HAOMs (Charlier et al., 2010), some of them dated to c. 1040 Ma (Bybee et al., 2014). The present work focuses on two older, fayalite-bearing, charnockitic intrusions, the Gloppurdi and Botnavatn intrusions, located in the granulite-facies country rocks of the RAP (Fig. 1). New field observations, geochemical data and U–Pb geochronological data are reported. They show that the rocks display major element compositions similar to the fayalite-bearing quartz mangerite of the Bjerkreim–Sokndal (BKSK) layered intrusion in the RAP, and trace element contents are comparable to Zr-rich jotunite, a rock type characteristic of AMCG plutonism. We conclude that these AMCG characteristics possibly link both intrusions to concealed anorthosite magma chambers at depth and underscore the episodic character of the AMCG plutonism in Rogaland. We propose that the Farsund Shear Zone (Bolle et al., 2010), which is well placed to have controlled emplacement of the RAP, was possibly active long before the main period of intrusion.

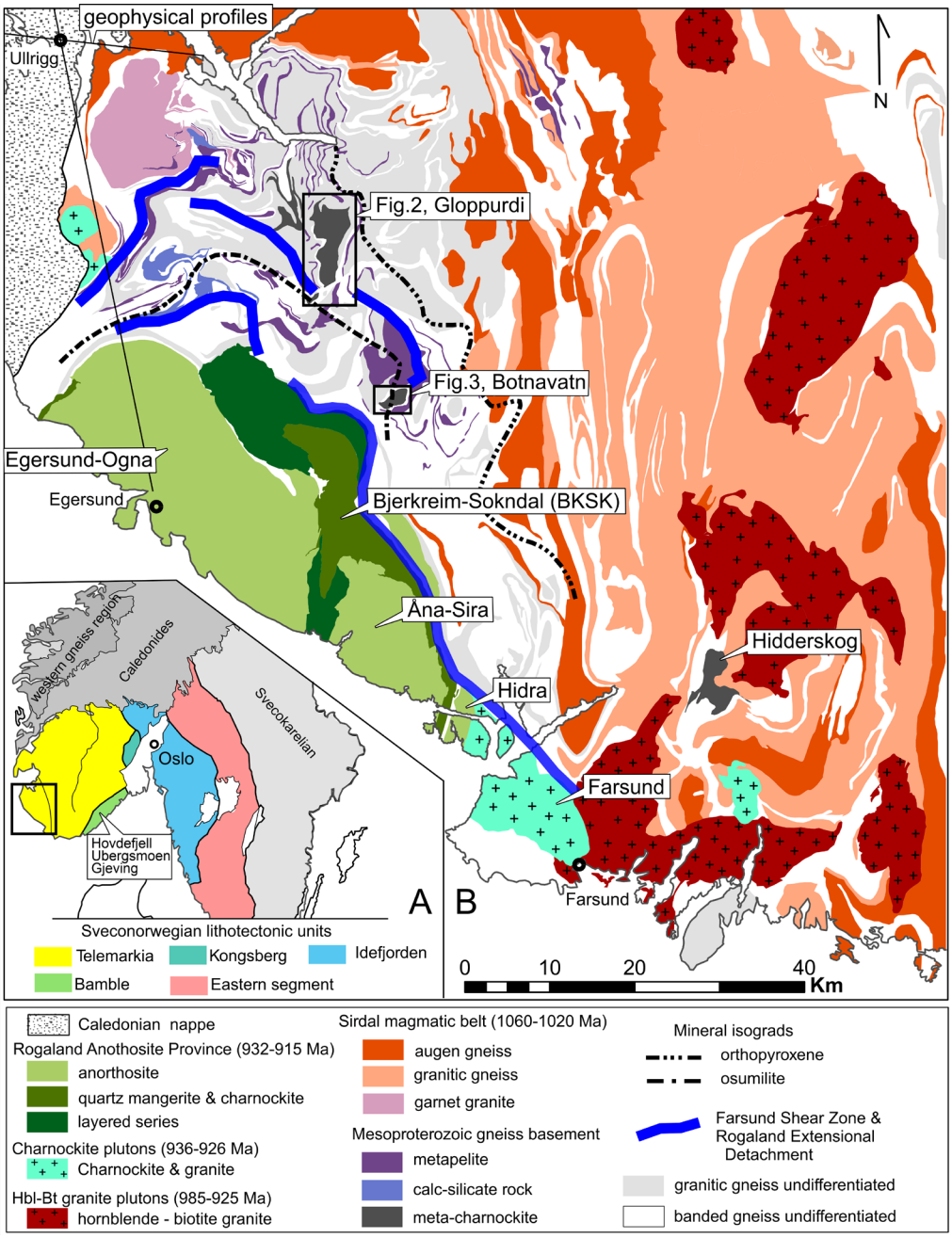

Figure 1. (A) Sketchmap of Sveconorwegian orogen. (B) Geological sketchmap of the Rogaland–Vest Agder area in South Norway following Laurent et al. (2018a) based on geological map by Falkum (1982) with information from Tobi et al. (1985; isograds), Marker et al. (2003; Rogaland Anorthosite Province), Bolle et al. (2010; Farsund Shear Zone), Coint et al. (2015; Sirdal Magmatic Belt) and Slagstad et al. (2022, Rogaland Extensional Detachment). Positions of the NNW–SSE and WNW–ESE profiles by Olesen et al. (2013) based on gravity and magnetic data and anchored at the Ullrigg borehole are shown. See text for references on geochronology.

Geological context

The regional geology in the Sveconorwegian orogen was recently reviewed in Slagstad et al. (2020) and Bingen et al. (2021). The Sveconorwegian orogeny itself can be interpreted as a continent-continent collision with the main orogenic phases between 1050 and 930 Ma (Moller & Andersson, 2018; Bingen et al., 2021) or alternatively as an accretionary orogeny controlled by a subduction zone lo-

cated to the west of the exposed orogen (Slagstad et al., 2020). Continental crust, in the Telemarkia lithotectonic unit (as defined by Bingen et al., 2005; Fig. 1), was accreted in a volcanic arc setting between c. 1520 and 1480 Ma. This event is well represented by the Suldal volcanic arc (Roberts et al., 2013). The juvenile crust was unconformably overlain by marine quartzite, known as the Seljord sequence in Telemark (Lamminen & Køykkä, 2010), and, between c. 1280 and 1140 Ma, by supracrustal rocks comprising bimodal (mafic-felsic) volcanic rocks and minor continental metasedimentary rocks (Lamminen & Køykkä, 2010). It was also intruded by plutonic rocks, dominated by A-type granites, characterized by a 'within-plate' geochemical signature (Andersen et al., 2009). Supracrustal rocks include the Saesvatn–Valldal supracrustal complex, and in Telemark, the Nissedal supracrustal complex and the Bandak sequence.

In Sveconorwegian times, the crust was shortened, thickened, folded and metamorphosed. The low-grade supracrustal rocks, representing the upper crust, are now exposed in synformal structures and exhibit partly preserved stratigraphic relations. The underlying gneissic and migmatitic complexes, representing the middle and lower crust, were affected by amphibolite- to granulite-facies metamorphism, mainly between 1050 and 930 Ma. This crust is intruded by voluminous plutonic complexes between 1060 and 900 Ma (Fig. 1): (i) the magnesian Sirdal magmatic belt (1060–1020 Ma) (Slagstad et al., 2013; Coint et al., 2015); (ii) the ferroan hornblende-biotite granite plutons (HBG, 985–925 Ma) (Vander Auwera et al., 2003; Andersen et al., 2007; Bingen et al., 2008; Slagstad et al., 2018; Wang et al., 2021); (iii) ferroan orthopyroxene and hornblende-biotite granite plutons (936–926 Ma), including the Farsund pluton (Vander Auwera et al., 2014*a*; Bolle et al., 2018); (iv) the Rogaland Anorthosite Province (RAP) (1041–915 Ma) (Schärer et al., 1996; Vander Auwera et al., 2011; Bybee et al. 2014); (v) granite pegmatite (923–893 Ma) (Müller et al., 2017), and (vi) the unfoliated WNW–ESE trending Hunnedalen jotunitic dyke swarm at 855 ± 59 Ma (Maijer & Verschure, 1998; Walderhaug et al., 1999).

In the gneiss complex, metamorphic grade increases south-westwards towards the RAP, perpendicular to the north–south trending and east-dipping regional fabric (Kars et al., 1980; Tobi et al., 1985; Maijer et al., 1987; Bingen & van Breemen, 1998; Laurent et al., 2018*a*, *b*; Slagstad et al., 2018; Slagstad et al., 2022; Fig. 1). Orthopyroxene-in and osumilite-in isograds are mapped (Tobi et al., 1985; Fig. 1). Osumilite is diagnostic of water-poor, ultrahigh temperature (UHT; T > 900°C) granulite-facies conditions (Harley, 2008). Petrological and geochronological data together provide evidence for protracted metamorphism peaking twice in low-pressure (4–6 kbar) UHT granulite-facies conditions, the first regional-scale event (referred to as M1) between c. 1030 and 1005 Ma, and the second (M2) between c. 940 and 930 Ma, associated with formation of osumilite (Tomkins et al., 2005; Drüppel et al., 2013; Blereau et al., 2017; Laurent et al., 2018*a*, *b*; Slagstad et al., 2018). Structural studies show that the metamorphic gradient is associated with a set of east-dipping extensional shear zones (top-to-east kinematics), collectively called the Rogaland Extensional Detachment (RED; Fig. 1), that resulted in exhumation of the highest-grade rock after c. 980 Ma (Slagstad et al., 2022). The concentric pattern of metamorphism therefore can not be interpreted as an aureole of contact metamorphism as proposed by Tobi et al. (1985).

The Rogaland Anorthosite Province (RAP)

The Rogaland Anorthosite Province (Fig. 1) consists of three large anorthosite massifs (Egersund–Ogna, Håland–Helleren and Åna–Sira massifs) and smaller leuconoritic bodies (Hidra and Garsaknatt intrusions) (Duchesne et al., 1985b; Vander Auwera et al., 2011). It also comprises the large Bjerkreim–Sokndal layered intrusion (BKSK; Wilson et al., 1996) that is made up of a series of anorthosite, troctolite, leuconorite, norite and gabbronorite cumulates. This layered series is topped by igneous quartz mangerite and charnockite among which fayalite-bearing quartz mangerite is considered as the residual liquid of the layered series (Duchesne & Wilmart, 1997; Vander Auwera et al., 2011).

A dyke system of jotunite, including Zr-rich jotunite, cuts across the whole province (Duchesne et al., 1985*a*; Duchesne & Liégeois, 2015). The three large anorthosite massifs are characterized by plagioclase with intermediate anorthite content (An_{40}–An_{55}). Geochemical and petrological arguments indicate that their parental magma is a high-alumina basalt, while the parental magma of the BKSK and Hidra intrusions is a jotunite (hypersthene monzodiorite) (Demaiffe & Hertogen, 1981; Duchesne & Hertogen, 1988; Vander Auwera & Longhi, 1994; Robins et al., 1997; Longhi et al., 1999; Charlier et al., 2010). All these rocks were intruded at a pressure of c. 5 kbar between c. 932 and 915 Ma (zircon and baddeleyite U–Pb data; Schärer et al., 1996; Vander Auwera et al., 2011).

High-alumina orthopyroxene megacrysts (HAOMs) hosted in the three large anorthosite massifs have Al_2O_3 content ranging from 2.3 to 8.5 wt.% (Charlier et al., 2010). The high Al content implies that HAOMs formed at a pressure of 10–13 kbar, deeper than the final pressure of c. 5 kbar of intrusion of the massifs (Longhi et al., 1999). It is therefore universally accepted that AMCG plutonism involves the development of a magma chamber at the boundary between the mantle and a thickened crust in which a high-alumina basalt coexists with HAOMs (Charlier et al., 2010). Models of polybaric intrusion of anorthosite plutons have been proposed, in which anorthosite plutons are rooted in a deep magma chamber and rose through the crust as a plagioclase-rich crystal mush (Charlier et al., 2010).

The origin of the basaltic magmas in anorthosite provinces is still debated. Following the model initiated by Emslie (1975), the high-alumina basalt has a mantle origin (Ashwal, 1993; McLelland et al., 2010; Bybee et al., 2014). Following the experimental work of Longhi et al. (1999), however, this magma is the product of remelting of a mafic source previously extracted from the mantle and stored near the mantle-crust interface (Schiellerup et al., 2000; Wiszniewska et al., 2002; Shumlyanskyy et al., 2006; Duchesne et al., 2007). Both models imply the development of UHT conditions at the base of the crust and production of felsic charnockite by contact anatexis (the Emslie model) and / or differentiation of ferromonzodioritic / jotunitic magma (the liquid line of descent (LLD) model of Vander Auwera et al., 1998).

Geology of the Gloppurdi and Botnavatn intrusions

The Gloppurdi and Botnavatn intrusions are hosted in the migmatitic granulite-facies gneiss complex between the orthopyroxene-in and osumilite-in isograds (Figs. 1–3). Their geology was first defined by Hermans et al. (1975), and subsequently by Rietmeijer (1979). The Gloppurdi intrusion forms the highest mountains in the area (Vinjakula) and occurs concordantly / interleaved within granulite-facies charnockitic migmatite (Fig. 2). It is a thick layer, some 10 km long, gently dipping (15–20°) to the east. The eastern border — the roof of the intrusion — is invaded by migmatitic gneiss and cannot be mapped accurately. The main rock in the intrusion is a strongly foliated, medium-grained, fayalite-bearing, felsic, mangerite to charnockite, with a characteristic pock-marked weathering surface, hereafter also called charnockitoid.

Finer-grained hololeucocratic layers or dykes, cross-cutting the foliation at low angles (<20°) or parallel with it, are ubiquitous (see below Fig. 4C). They range in thickness from a few centimetres to several decimetres. Melanocratic rocks are interleaved as layers, lenses or locally as enclaves. A hololeucocratic felsic dyke occurs close to the roof of the intrusion.

The smaller (some 4 km long) Botnavatn intrusion is also dominated by fayalite-bearing charnockite, concordantly interleaved with charnockitic migmatite (Rietmeijer, 1979) (Fig. 3). The rocks are foliated, also showing a pock-marked appearance.

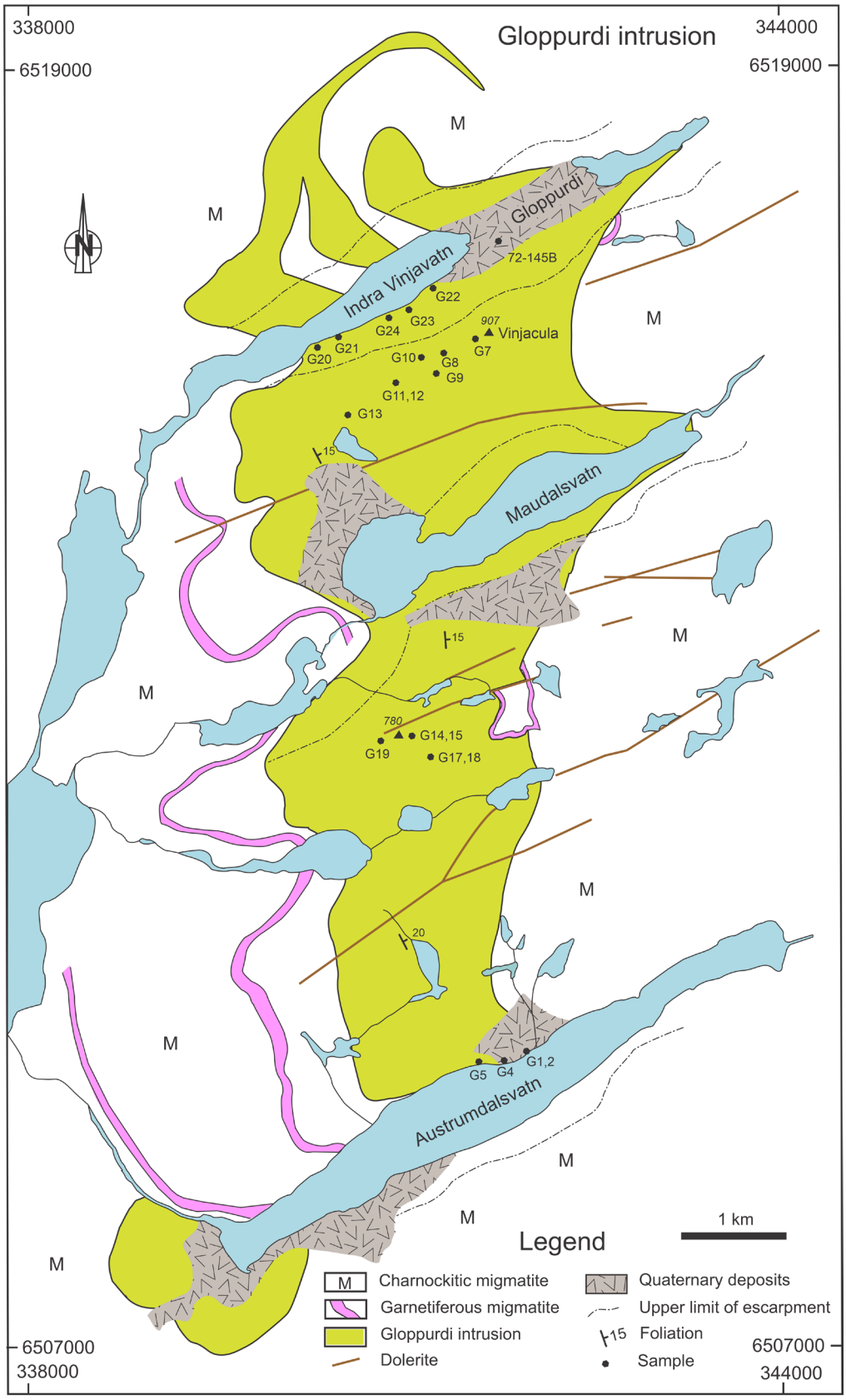

Figure 2. Geological sketch map of the Gloppurdi intrusion (after Rietmeijer, 1979) with location of samples.

Published geochronology on the Gloppurdi intrusion includes a whole-rock Rb–Sr isochron age of 1180 ± 70 Ma (Versteeve, 1975), and a zircon U–Pb age of 1233 ± 42 Ma from a sample (RO98B–2001) collected in the Gloppurdi rock avalanche field (Slagstad et al., 2018; Fig. 2; same locality as sample 72–145B of this study). For Botnavatn, a zircon U–Pb upper-intercept date of 1060 ± 15 Ma was published by Wielens et al. (1980). However, this date is obtained from non-abraded multigrain zircon fractions and is unreliable. Both intrusions have been deformed during the M1 metamorphic event.

Sampling and petrography

Twenty-eight samples were collected (Figs. 2 & 3). Their petrography is summarised in Electronic Supplement Table S1. Fayalite-bearing charnockitoid is the dominant type. It shows a typical greenish-brown colour and is made up of quartz (with fluid inclusions), microperthitic to mesoperthitic K-feldspar, plagioclase, fayalite, clinopyroxene, traces of orthopyroxene, apatite, Fe–Ti oxides and zircon. The mafic minerals form clusters elongated in the foliation plane (Figs. 4C & 5A). In some specimens, the mafic minerals can be altered, giving the rock a whitish colour. Following the nomenclature of charnockitic rocks (Streckeisen, 1974; Le Bas et al., 1986; Fig. 6D), they vary from mangerite (#G9, G11, G15), quartz mangerite (#G1, G19, G21, G23, 72–145B) to charnockite (*sensu stricto*) (#G2, G5). Some rocks are devoid of fayalite: samples #G20 and #G6 are quartz mangerite and #G24 is a charnockite.

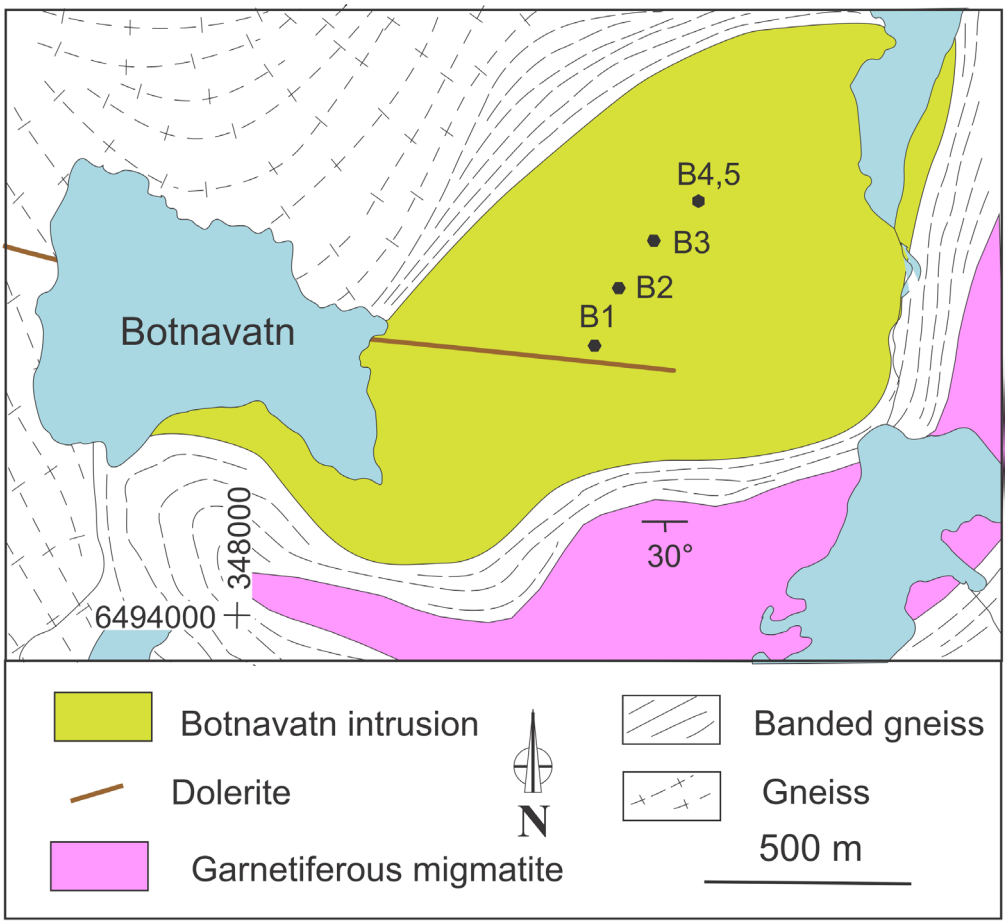

Figure 3. Geological sketch map of the Botnavatn intrusion with location of samples.

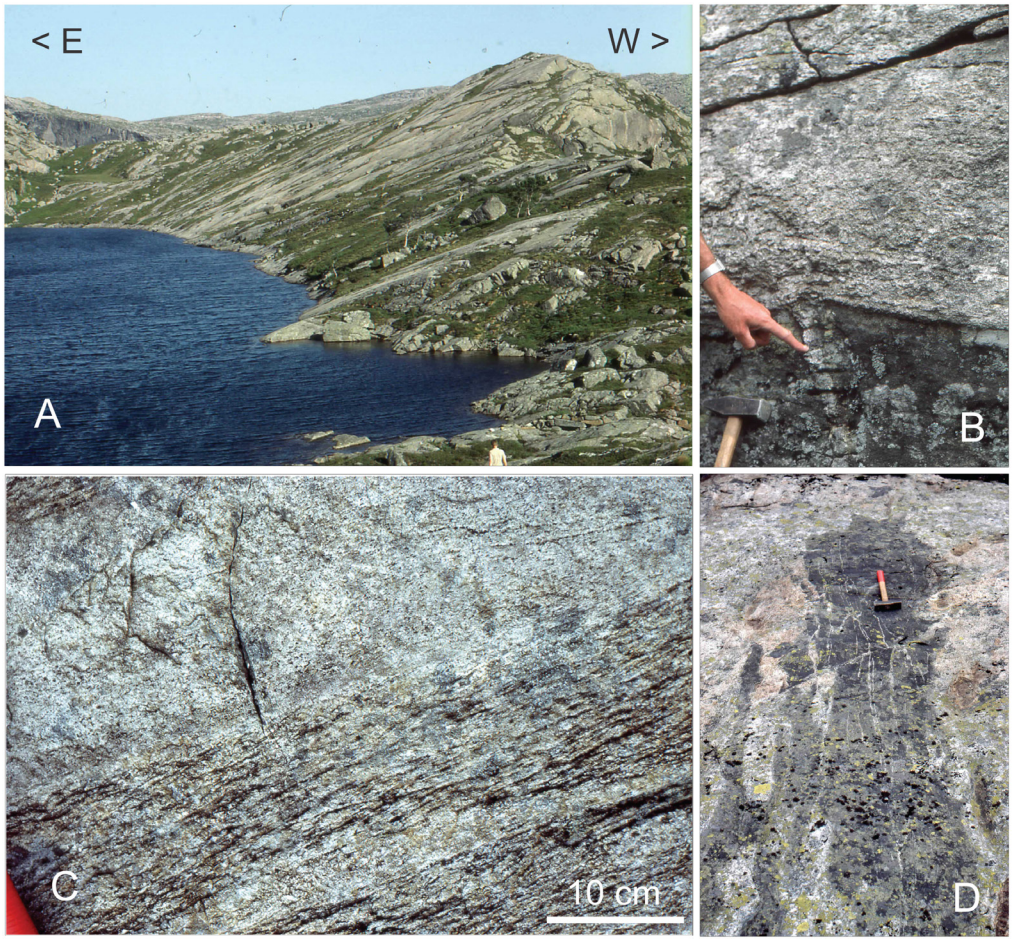

Figure 4. (A) East dipping (20°) gneissic foliation in the Gloppurdi intrusion. (B) Contact between charnockitic and mafic layers. The finger indicates a subvertical 3 cm-thick granitic dykelet cutting across the mafic rock. (C) Contact between fine-grained charnockitic dykes and fayalite-bearing charnockitoid at a small angle to the foliation. (D) Foliated mafic enclave invaded / dissected by quartzofeldspathic melt at dm- and cm-scales.

The fine-grained (<1 mm) leucocratic layers or dykes that crosscut the foliation at low angles are common (#G12, G13, G14, G18, G22; Fig. 4C). They show a foliation underlined by mafic mineral strings and elongated crystals of quartz and feldspars (Fig. 5C). They are made up of quartz, antiperthitic plagioclase, microperthitic orthose or mesoperthite with subordinate amounts of mafic minerals. The latter may include subhedral grains of biotite (#G22) or amphibole (#G12, #G13) that also occur as alteration products of pyroxenes. Traces of euhedral Fe–Ti oxides, apatite and zircon are ubiquitous. Myrmekite is frequent in the plagioclase-bearing samples. When included in the microperthite, the plagioclase grains show an albite rim.

Although orthopyroxene is not present in #G14 and #G18 (fine-grained dykes), feldspar in these samples is mesoperthitic, typical of charnockites and dry hypersolvus granites (Streckeisen, 1974, 1976). We therefore consider that these samples belong to the charnockite family.

The mafic rocks are biotite-bearing amphibolite occurring as enclaves (#G8, #G10) or metre-thick layers (#G17). Locally, quartzo-feldspathic veins are present in the mafic rocks (Fig. 4B, D). A foliated amphibole-bearing quartz monzonite dyke (#G4), oblique to the main foliation, was sampled in the Austrumdalsvatn section (Fig. 2) as was a hololeucocratic leucocharnockite dyke (#G7) close to the roof of the intrusion at the top of the mountain Vinjacula (Fig. 2).

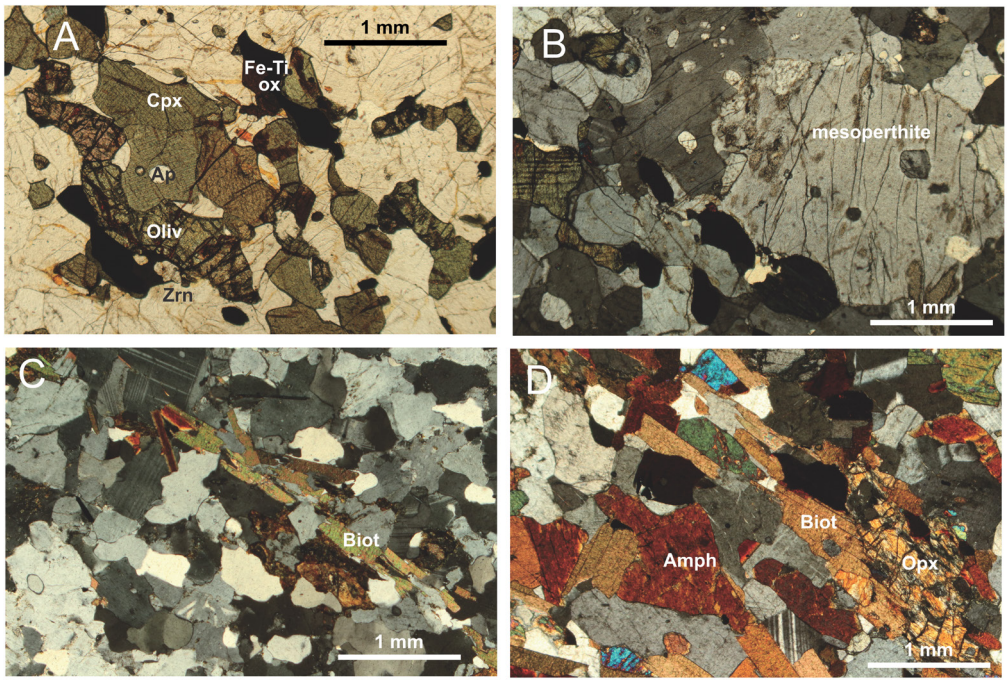

Figure 5. Photomicrographs. (A) Cluster of mafic minerals including fayalite olivine (Oliv), clinopyroxene (Cpx), Fe–Ti oxides (Fe–Ti ox), apatite (Ap), zircon (Zrn) in fayalite-bearing mangerite sample #G9. The cluster is oriented parallel to the foliation (plane-polarized light). (B) Mesoperthitic feldspar enclosing plagioclase grains in sample #G9 (cross-polars light). (C) Biotite-bearing fine-grained charnockitic dyke, sample #G22. Note the sub-granular structure with elongated grains parallel to a foliation marked by biotite (Biot) flakes (cross-polars light). (D) Biotite- and orthopyroxene-bearing amphibolite sample #G10 (cross-polars light) (orthopyroxene: Opx, biotite: Biot, amphibole: Amph).

In Botnavatn (Fig. 3), the felsic charnockitoids are fayalite-bearing (#B1 quartz mangerite, #B2 charnockite) or devoid of fayalite (#B3, B4). Mafic layers (locally crosscut by granitic dykelets, Fig. 4B) are biotite-amphibolite with orthopyroxene and opaque minerals (#B5).

Geochemistry

Whole-rock major element analyses were performed by XRF on an ARL 9400 XP spectrometer on lithium tetra- and metaborate glass discs (FLUORE-X65®), with matrix corrections following the Traill-Lachance algorithm (ARL). Rb, Sr, Ba, Y, Zr, Nb, Pb, and Zn were analysed on pressed powder pellets by XRF. Neutron-activation analyses of REE, U, Th, Ta, Hf, Sc, Co and Cs were carried out in the Pierre Sue Laboratory (CEN, Saclay, France) following the method described by Jaffrezic et al. (1980). Zr was analysed by both XRF and neutron activation to confirm for the absence of nugget effect in Zr XRF determination. Results by the two methods are comparable.

The analyses are reported in Electronic Supplement Table S2. In the classification diagrams of Frost et al. (2001), all felsic rocks are ferroan (except #G22) (Fig. 6B), most fayalite-bearing charnockitoid samples are alkalic and the fine-grained dykes are alkali-calcic (Fig. 6A). In the Shand diagram, all felsic rocks have Al / (Ca + Na + K) ratios lower than 1.1 (Fig. 6C). In Harker diagrams for major elements (Fig. 7), the mafic rocks from Gloppurdi and Botnavatn show the same composition, the enclave #G8 being somewhat richer in SiO2, possibly due to contamination by acidic melts. The felsic charnockitoid samples vary from 60 to 72% SiO_2 and the fine-grained dykes cluster around 72% SiO_2, both rock types being mostly very-high K (Fig. 7H). A notable feature is the low Mg# or high Fe* (Mg# < 0.1

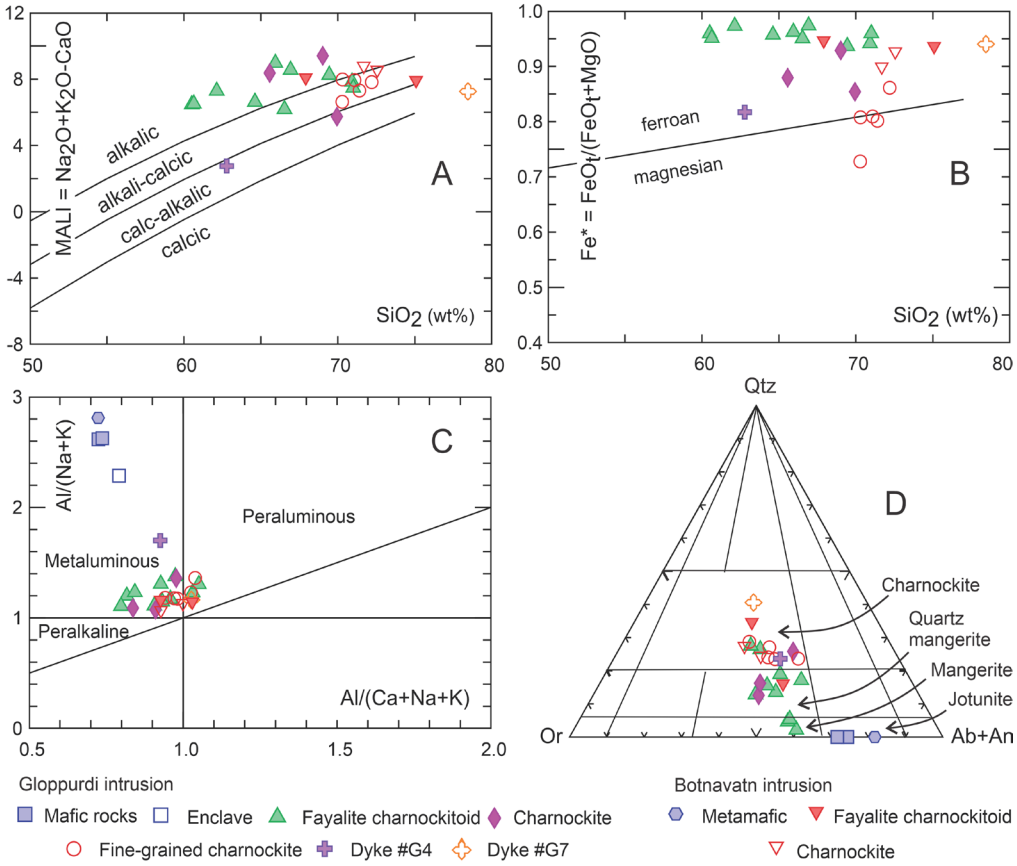

Figure 6. Major element compositions of the different rock types in the Gloppurdi and Botnavatn intrusions in classification diagrams. (A & B) MALI (Na2O + K2O–CaO) and Fe (FeOt/(FeOt + MgO)) vs. SiO2 by Frost et al. (2001); (C) Shand diagram (Al / (Na + K) vs. Al / (Ca + Na + K)); D: Normative Or–Qtz–Ab + An triangular diagram for charnockitic rocks after Streckeisen (1976).*

with Mg# = (MgO / (FeOt + MgO) or Fe* > 0.9 with Fe* = (FeOt / (FeOt + MgO)) (Figs. 6B & 7D) in the fayalite-bearing charnockitoid and the higher Mg# in the fine-grained dykes (up to 0.4). In Harker diagrams for trace elements (Fig. 8), Zr, Th, U, Ta, Ce and Y may reach high values in the fayalite-bearing charnockitoid, particularly in the low silica samples. Therefore, these rocks classify as A-type granitoid following Whalen et al. (1987). The fine-grained dykes are remarkably high in Sr (Fig. 8G) compared to the fayalite-bearing charnockitoid. The REE distributions are relatively high in the fayalite-bearing charnockitoid (Fig. 9A) with an average $(La / Yb)_n$ = 7 and a negative Eu anomaly (average Eu / Eu* = 0.59). By contrast, in the fine-grained dykes (Fig. 9B), the REE are lower, with a larger $(La / Yb)_n$ = 34 and no systematic Eu anomaly (average Eu / Eu* = 0.98). A characteristic trait of the fayalite-free charnockite is the low REE contents with positive Eu anomaly (Fig. 9C). The hololeucocratic dyke (#G7) reaches 78% SiO_2 with minimum values of most elements (Figs. 7 & 8). The REE contents (Fig. 9D) are very low and the distribution shows a strong positive anomaly (Eu / Eu* = 3.1) and a moderate (La / Tb)n ratio (17). The mafic rocks display low REE contents (Fig. 8I, J) and flat distributions (Fig. 9E) with insignificant Eu anomaly.

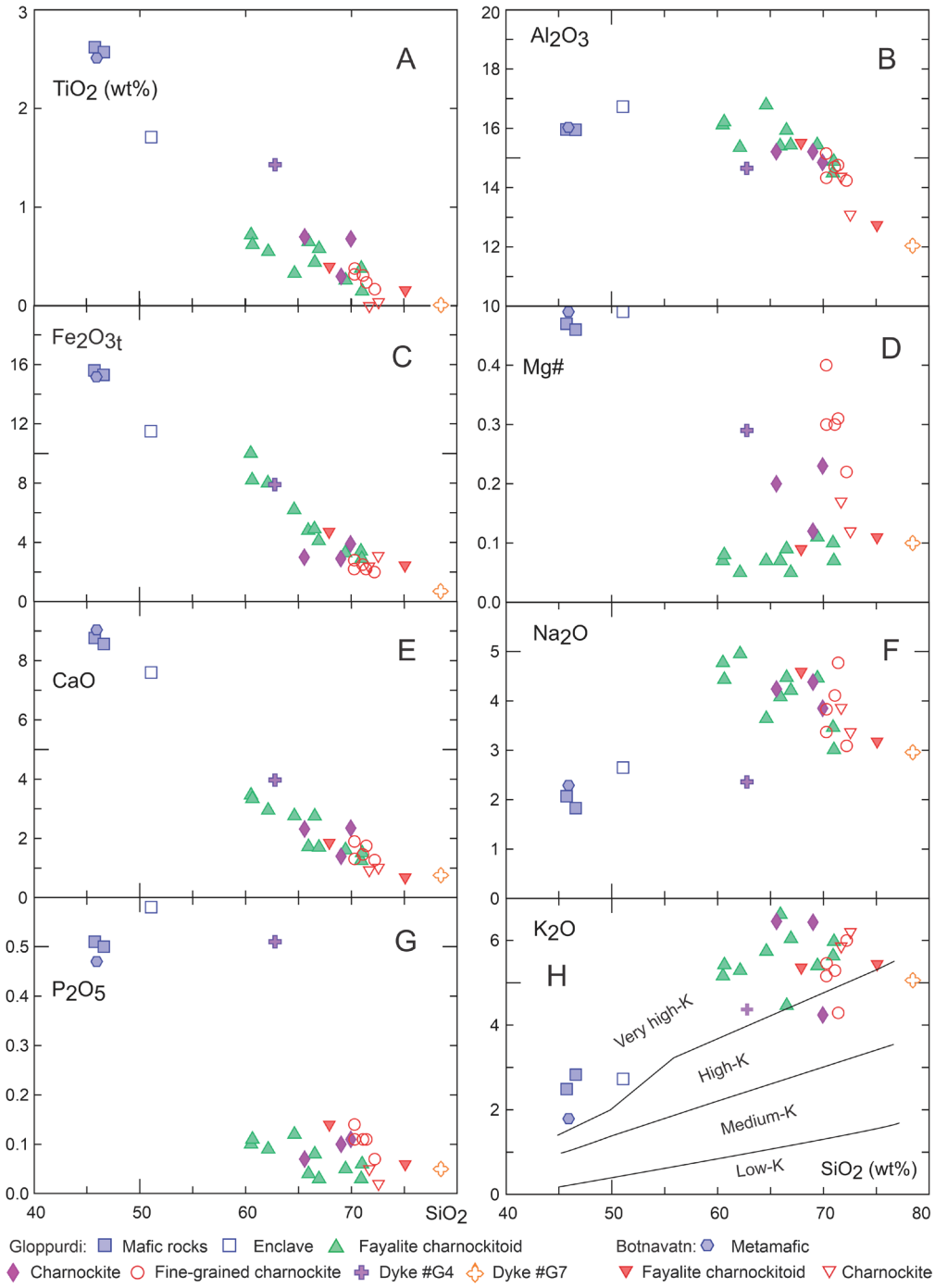

Figure 7. (A–H) Harker diagrams showing major element compositions (wt.%) of the Gloppurdi and Botnavatn intrusions. (H) divisions following Peccerillo and Taylor (1976).

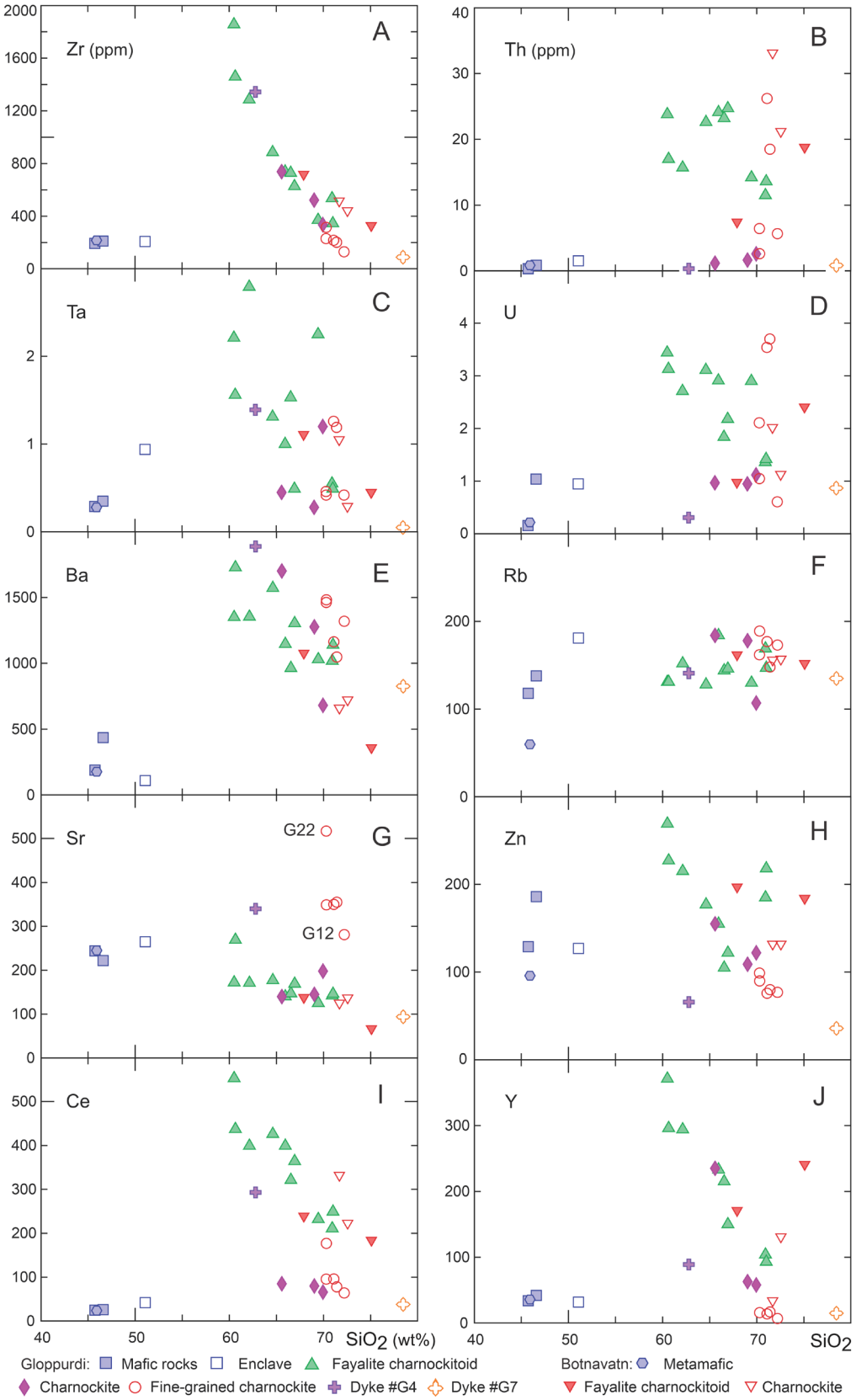

Figure 8. (A–J) Harker diagrams for significant trace element compositions (ppm).

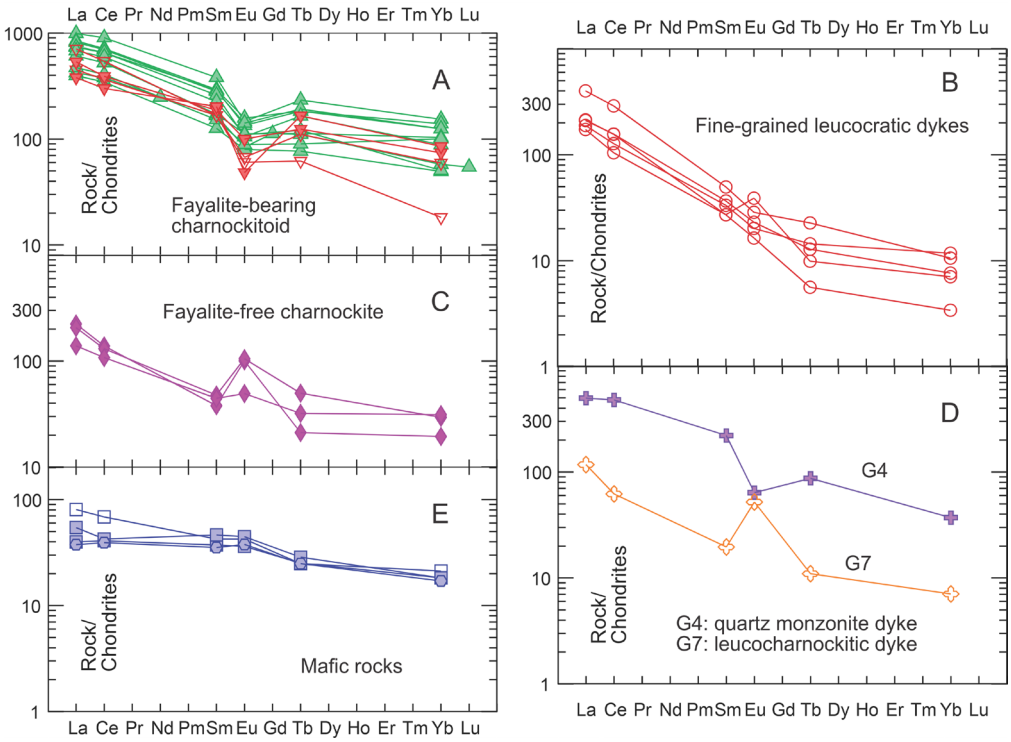

Figure 9. (A–D) Chondrite-normalized REE distributions. Normalizing values after Sun and McDonough (1989).

Zircon U–Pb geochronology

Zircon was separated using conventional mineral separation methods from crushed samples. Clear zircon crystals were hand-picked in alcohol, mounted in epoxy, polished and imaged in a scanning electron microscope with cathodoluminescence (CL) and backscattered electron (BSE) detectors. U–Pb data were collected by laser ablation inductively coupled plasma mass spectrometry (LA–ICPMS) at the MIMAC laboratory, Geological Survey of Norway. Zircon samples and standards were ablated in a He atmosphere with a Teledyne - Photon Machines Analyte Excite 193 nm excimer laser, using a circular beam aperture to obtain 'spot analyses' of c. 15 µm in diameter. The fluence for the spot analyses was set to 2 J/cm^2 with a repetition rate of 6 Hz. The laser is connected to a Nu Plasma 3 multi-collector ICP–MS, where ^{206}Pb and ^{207}Pb are measured on Daly detectors, while ^{202}Hg, ^{204}(Pb + Hg), ^{208}Pb are measured using ion counters and ^{238}U and ^{232}Th are measured on Faraday cups. The sampling time was 30 seconds with on-peak baseline measurements of 20 seconds. The GJ–1 zircon (602 Ma) was used as a primary standard (Jackson et al., 2004), and analysed between every 5 analyses of unknowns. The zircons 91500 (1065 Ma, Wiedenbeck et al., 1995), Plešovice (337 Ma, Slama et al., 2008) and Z6412 (1160 Ma, GSC Ottawa, unpublished) were used as secondary standards, inserted at regular intervals in the analytical session, to monitor the quality of analyses. Data reduction was performed with the IOLITE v.4 software which includes baseline calculation, down-hole fractionation correction, selection of consistent segments of signal and error propagation (Paton et al., 2011; Petrus and Kamber, 2012). No common Pb correction was performed on the analyses. However, 202Hg and 204(Hg + Pb) were analysed and portions of analyses or analyses containing detectable common Pb were filtered away. Error propagation includes propagation of internal and external uncertainties. The analytical procedure is summarized in Electronic Supplement Table S3 (including values for secondary standards) and the data are reported in Electronic Supplement Table S4, with propagated 2 sigma uncertainty, and in Fig. 10.

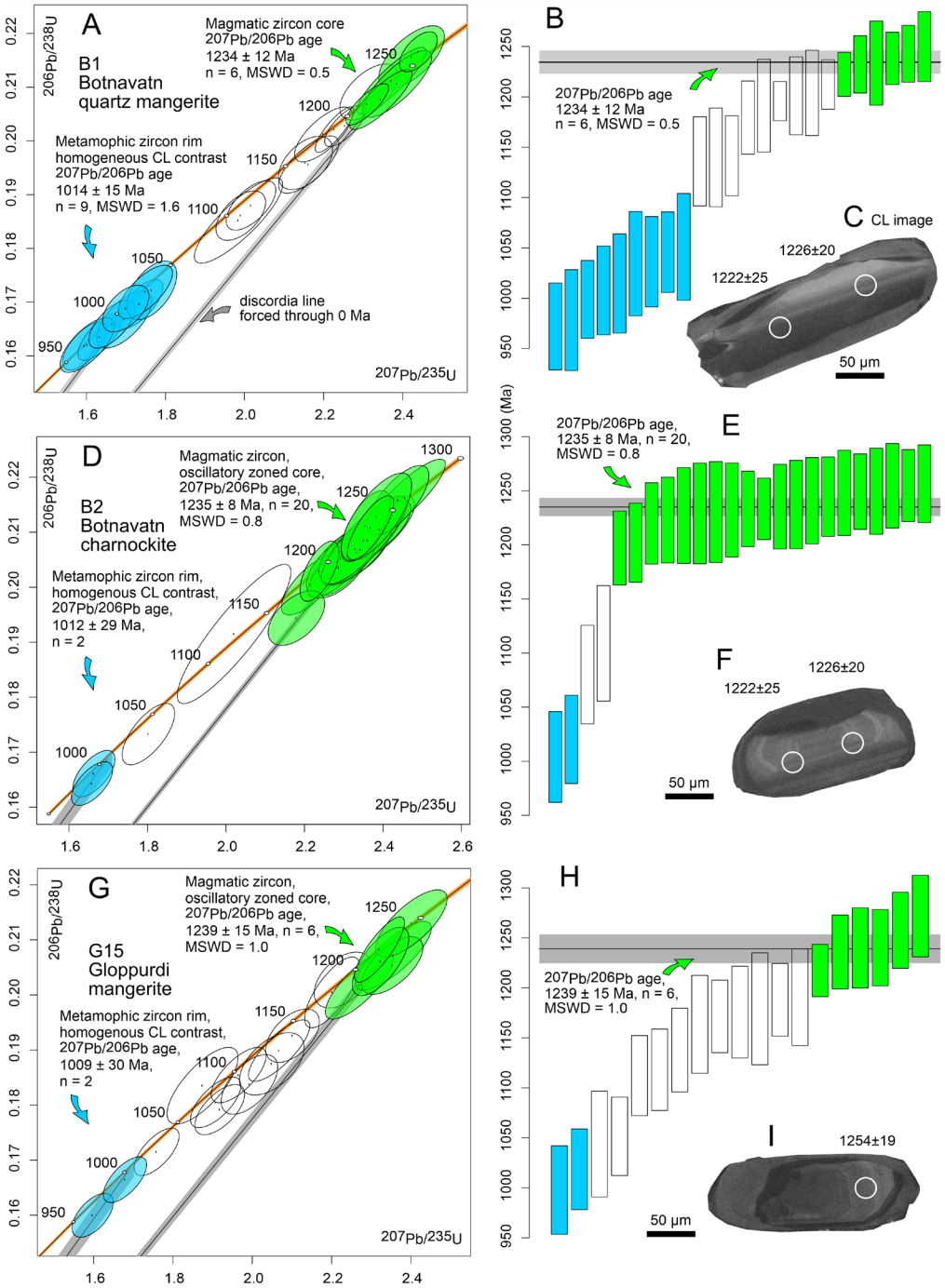

Figure 10. Zircon U–Pb geochronological data and selected cathodoluminescence (CL) images of zircon with position of analyses. (A–C) quartz mangerite sample #B1, Botnavatn; (D–F) charnockite sample #B2, Botnavatn; (G–I) mangerite sample #G15, Gloppurdi.

Three samples were dated: a quartz mangerite (#B1) and a charnockite (#B2) from Botnavatn (Fig. 3) and a mangerite (#G15) from Gloppurdi (Fig. 2). The samples contain abundant prismatic and rounded zircon crystals with length commonly above 200 µm. Two zones are clearly identified on CL images (Fig. 10): variably oscillatory zoned zircon generally forming a core, and zircon with homogeneous dark grey CL contrast generally forming a rim. Some prismatic well-terminated automorphic zircon crystals show a rounded oscillatory zoned core surrounded by a prismatic rim with homogeneous CL contrast or are entirely made of zircon with homogeneous CL contrast. This morphology suggests that

the zircon with homogeneous CL contrast crystallized inwards at the expense of the oscillatory zoned zircon and does not represent an overgrowth. The oscillatory zoned core is best preserved in the silica-rich charnockite (#B2). Oscillatory zoned zircon is interpreted as magmatic while the zircon with homogeneous CL contrast is interpreted as metamorphic.

The 3 samples show similar geochronological results (Fig. 10). In each sample, a group of analyses of cores define an old age of c. 1236 Ma (^{207}Pb / ^{206}Pb age) and a second group of analyses on zircon with dull homogeneous CL contrast define a younger age of c. 1013 Ma. A third group, generally on cores with poorly defined zoning, range between the two first groups with intermediate ^{207}Pb / ^{206}Pb apparent age, asymptotic towards the old age. Zircon in the three age groups is characterized by similar Th / U ratio (average values of 0.64, 0.64 and 0.67 for groups 1 to 3 respectively).

The group of analyses at c. 1236 Ma is interpreted to date magmatic crystallization of the rocks, while the group at c. 1013 Ma is interpreted to date metamorphism. The third group represents magmatic zircon affected by partial recrystallization or partial radiogenic lead loss. In more detail (Fig. 10), the three samples yield overlapping ^{207}Pb / ^{206}Pb ages for the magmatic event at 1234 ± 12 Ma (n = 6, MSWD = 0.5) for quartz mangerite #B1, 1235 ± 8 Ma (n = 20, MSWD = 0.8) for charnockite #B2, and 1239 ± 15 Ma (n = 6, MSWD = 1.0) for mangerite #G15. The three samples also yield overlapping ^{207}Pb / ^{206}Pb ages for the metamorphic event at 1014 ± 15 Ma (n = 9, MSWD = 1.6) for quartz mangerite #B1, 1012 ± 29 Ma (n = 2) for charnockite #B2, and 1009 ± 30 Ma (n = 2) for mangerite #G15. These dates indicate that the two intrusions are part of the same magmatic event at 1236 ± 8 Ma (pooled weighted average ^{207}Pb / ^{206}Pb age, n = 31, MSWD = 0.8), corroborating the age of 1233 ± 42 Ma by Slagstad et al. (2018). They were both affected by a common metamorphic event at 1013 ± 12 Ma (n = 13, MSWD = 1.1), inside the time interval for the well-established M1 regional metamorphic event peaking in granulite-facies conditions in Rogaland (Tomkins et al., 2005; Drüppel et al., 2013; Laurent et al., 2018*a*, *b*).

Genesis of the Gloppurdi and Botnavatn intrusions

Fayalite-bearing charnockitoid

Fayalite-bearing charnockitoid is the most abundant and characteristic rock type in the Gloppurdi and Botnavatn intrusions. In the classification diagrams of Frost et al. (2001), this rock type is characterized by an alkalic signature with low Mg# (Mg# < 0.1; Fig. 11). At the regional scale in South Norway (Fig. 1), it is distinctly more alkalic than the calc-alkalic to alkali-calcic trends of the Hidderskog, Gjeving and Hovdefjell charnockitic intrusions formed at c. 1160–1140 Ma (Zhou et al., 1995; Bingen & Viola, 2018) and the charnockitic facies of the Farsund pluton formed at c. 930 Ma (Bolle et al., 2010; Vander Auwera et al., 2014*a*; Fig. 11). Its combined alkalic and low Mg# signature is similar to that of the quartz mangerite of the BKSK layered intrusion in the RAP, especially the fayalite-bearing quartz mangerite (Fig. 11). This group of rocks is known as the olivine-bearing trend (OLT) or fayalite-bearing trend (Duchesne & Wilmart, 1997; Bolle & Duchesne, 2007; Fig. 11). In the BKSK intrusion, the fayalite-bearing quartz mangerite lies on top of layered norite and is considered to result from the fractional crystallization of a jotunitic parental magma with some assimilation of country rocks (Nielsen et al., 1996; Duchesne & Wilmart, 1997; Vander Auwera et al., 2011).

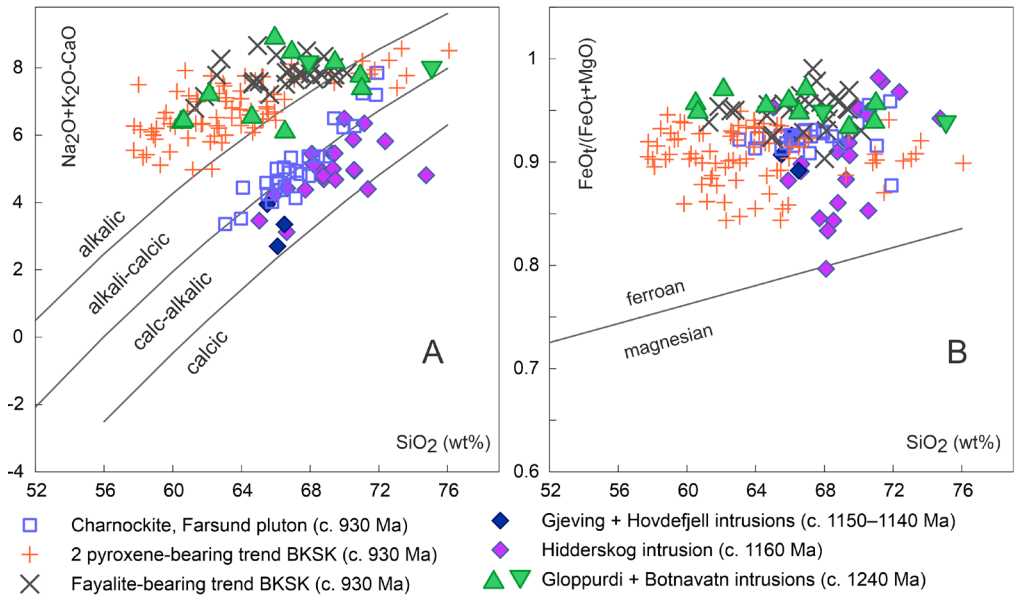

Figure 11. (A & B) Classification diagrams by Frost et al. (2001) comparing the fayalite-bearing charnockitoid of Gloppurdi and Botnavatn to other charnockitic intrusions in South Norway, including the Hidderskog, Gjeving and Hovdefjell intrusions (Zhou et al., 1995; Bingen & Viola, 2018), the charnockitic facies of the Farsund pluton (Bolle et al., 2010; Vander Auwera et al., 2014a), and the quartz mangerite of the BKSK layered intrusion, including the 2 pyroxene-bearing trend and fayalite-bearing trend (Duchesne & Wilmart, 1997; Bolle et al., 2003).

Fig. 12 shows the overlap of major elements between the fayalite-bearing charnockitoid from Gloppurdi and Botnavatn and the fayalite-bearing trend from BKSK. Significant differences, however, appear when the trace elements are considered (Fig. 13). In the fayalite-bearing charnockitoid from Gloppurdi and Botnavatn, Zr is more variable and may reach high values (Fig. 13A), Th, U, and Ce are on average higher than the fayalite-bearing trend in BKSK (Fig. 13B–D), and the REE distributions show higher values and larger negative Eu anomalies (Fig. 13 D–F).

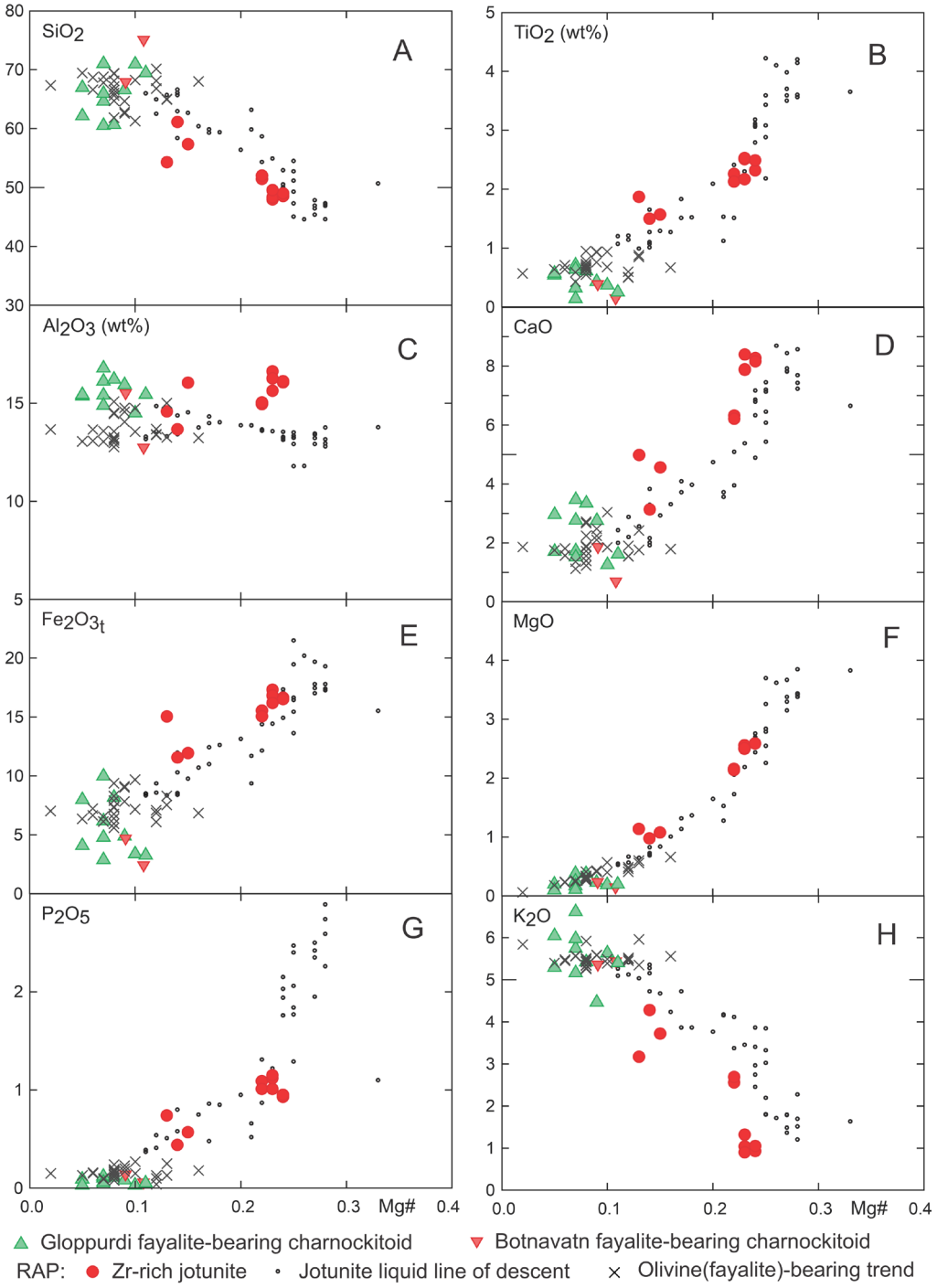

Figure 12. (A–H) Variation diagrams of major elements (wt.%) vs. Mg#, comparing the fayalite-bearing charnockitoid of Gloppurdi and Botnavatn to (1) the fayalite-bearing trend (OLT) of the BKSK layered intrusion (Duchesne & Wilmart, 1997); (2) the jotunitic liquid line of descent in the RAP (Vander Auwera et al., 1998); (3) the Zr-rich jotunite in the RAP (Duchesne & Liégeois, 2015).

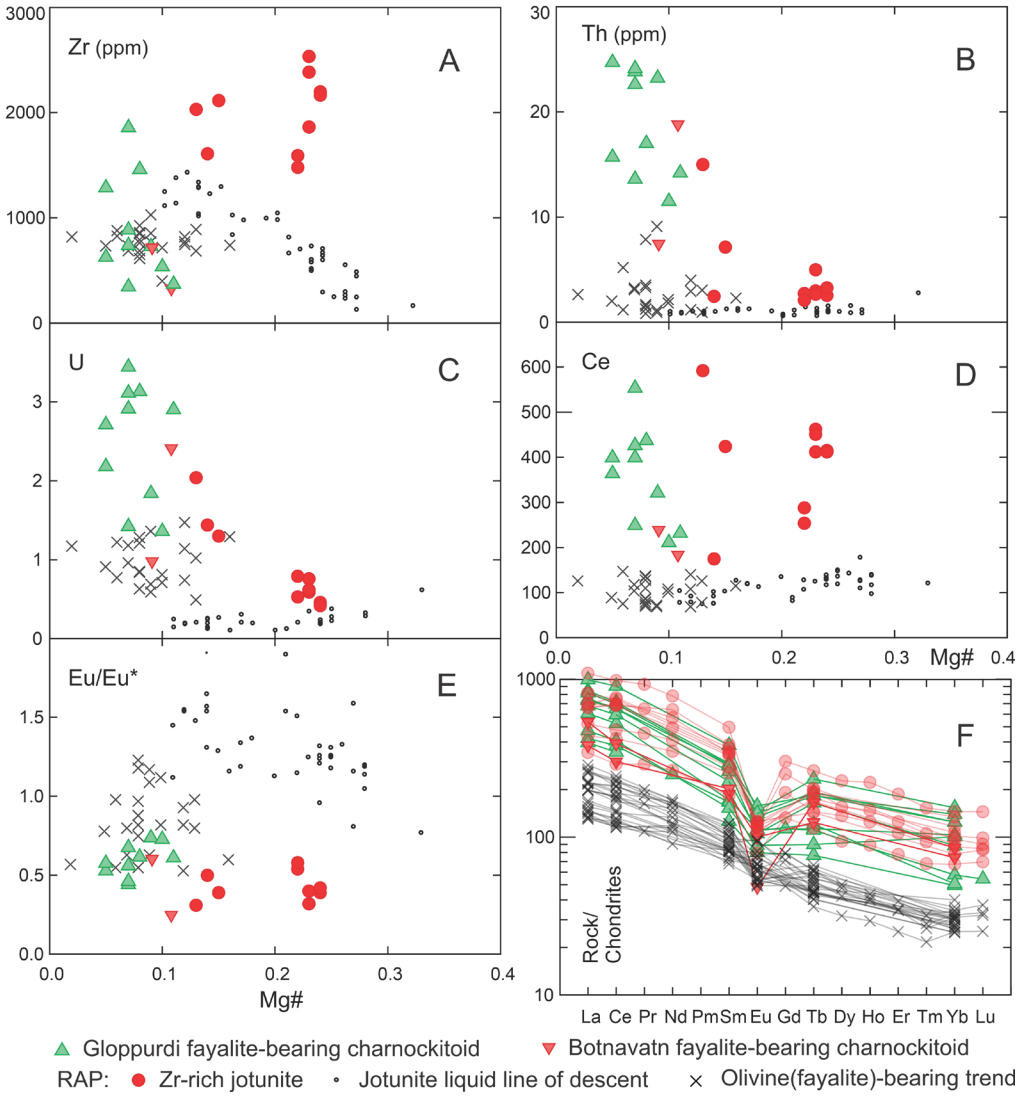

Figure 13. (A–E) Variation diagrams for significant trace elements (ppm) vs. Mg#. (F) chondrite-normalized REE diagram comparing the fayalite-bearing charnockitoid of Gloppurdi and Botnavatn to the fayalite-bearing trend of the BKSK intrusion (Duchesne & Wilmart, 1997) and to Zr-rich jotunite (Duchesne & Liégeois, 2015).

Variations within the group

A challenging property of the fayalite-bearing charnockitoid is the large variation of the SiO_2 content (Fig. 7) from 60% to 71% in Gloppurdi and from 68% to 75% in Botnavatn, a variation correlated to Zr, U, Th, Ta, REE, Ba, and Zn (Fig. 8). This variation cannot be explained by density-controlled fractional crystallization because of the small variation of the Mg# (from 0.05 to 0.10). We suggest that it is due to a mixing process between an end-member made up of quartzo-feldspathic minerals and another end-member made up of all mafic minerals together. This mixing is suggested by a linear array in the triangular diagram of Fig. 14 and by the observation under the microscope of the grouping of mafic minerals in clusters (Fig. 5A). High correlation factors between TiO_2 and Zr (0.78) suggest that zircon belongs to the mafic minerals group, and high correlation factors between Zr and Nb (0.90), and Ce (0.88) show that the mafic pole controls the distribution of these elements. U and Th have low correlation factors with Zr, implying a control by other minerals. Variations in compositions between two end-members has been documented in the BKSK noritic cumulates (Duchesne & Charlier, 2005) and attributed to variable nucleation rate of the plagioclase rather than to density-controlled crystal sorting,

because the mafic pole comprises minerals of very contrasting densities. It is thus suggested here that variable nucleation rates of the quartzofeldspathic minerals also explain the differentiation within the fayalite-bearing charnockitoid group.

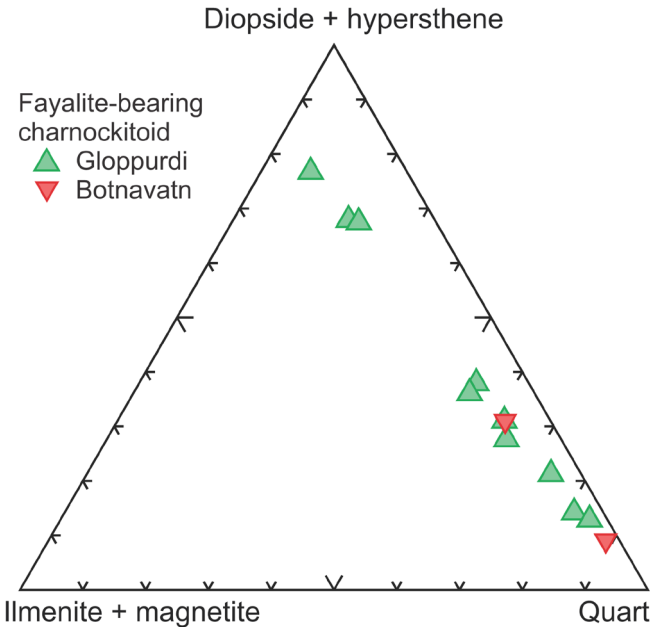

Figure 14. Normative composition of the fayalite-bearing charnockitoid in Gloppurdi and Botnavatn projected in the triangular diagram ilmenite + magnetite – diopside + hypersthene – quartz.

Similarity with Zr-rich jotunite (ferromonzodiorite) in AMCG complexes

Although the exact composition of undifferentiated fayalite-bearing charnockitoid cannot be determined, differentiation diagrams (Figs. 12 & 13) show that this group plots in the continuation of the Zr-rich jotunite / ferromonzodiorite trend towards low Mg# values, as defined by Duchesne and Liégeois (2015), and can thus belong to this family. The saturation temperature of zircon, following Boehnke et al. (2013), ranges from 802°C to 924°C (Electronic Supplement Table S2). The undifferentiated compositions had thus a temperature within this range and resulted from the evolution of a parental magma at even higher temperatures, in UHT conditions (>900°C). The Zr-rich jotunite is a relatively rare rock that has been identified in well-studied anorthosite provinces such as the Laramie Anorthosite Complex (Wyoming) (Mitchell et al., 1996; Scoates & Chamberlain, 2003), the Adirondack mountains (Grenville orogen, USA) (Seifert et al., 2010), or the RAP (Duchesne & Liégeois, 2015). In the last province, this rock type is well documented. It defines a coarse evolution trend parallel to the jotunitic liquid line of descent (Vander Auwera et al., 1998; Figs. 12 & 13) and can thus be explained by a similar fractional crystallization process. Duchesne and Liégeois (2015) proposed that the parental melt of the Zr-rich jotunite is a Fe-rich basaltic melt resulting from an immiscibility process at a 6–13 kbar pressure range, deeper than the emplacement of the anorthosites (c. 5 kbar). It is noticeable that the immiscible Fe-rich melt can concentrate not only Zr and REE but also U and Th.

In conclusion, the peculiar compositions of the fayalite-bearing charnockitoid in the Gloppurdi and Botnavatn intrusions support their origin as differentiated products of Zr-rich jotunite / ferro-monzodiorite related to AMCG magmatism.

Fayalite-free charnockitoid

Some of the charnockitic rocks are devoid of fayalite. Samples #G6 and #G20 are quartz mangerite and #G24 is a charnockite (Fig. 6D). They plot at the end of the fayalite-bearing charnockitoid trend in Harker diagrams (Figs. 7 & 8). Nevertheless, they show higher values of Mg# (Fig. 7D). Their typical feature is a relatively low REE content with a positive Eu anomaly (Fig. 9C). This characteristic can be explained by accumulation of feldspar, and we consider that these rocks are feldspar-laden magmas.

Fine-grained charnockite

In Harker diagrams, the fine-grained charnockite (#G12, G13, G14, G18, G22) plots close to 71% SiO2 at the end of the general trend for most elements (Fig. 7). However, it shows Mg# that vary from 0.2 up to 0.4 (Fig. 7D) and Sr concentrations up to 517 ppm (#G22 in Fig. 8G) in clear contrast to other charnockitic rocks at the same SiO2 content. Could the high Sr content of the fine-grained charnockite correspond to plagioclase-laden magmas? Plagioclase, as observed for instance in the BKSK intrusion (Roelandts & Duchesne, 1979; Charlier et al., 2005), shows a large positive Eu anomaly. Addition of plagioclase to sample #G12 (Eu / Eu* = 1.8; Electronic Supplement Table S2) to obtain #G22 (Fig. 8G) would increase this ratio, a fact not observed in G22 in which the Eu / Eu* ratio is 0.8; Electronic Supplement Table S2). This scenario is thus not realistic. In fact, relatively high Sr content and high Mg# in granite suites are not rare in nature. Our Sr-rich charnockite showing A / CNK < 1.10 (Fig. 6C) can be considered as I-type granite (Chappell, 1999). According to Whalen et al. (1987), I-type granite on average shows high Sr concentration with a large interval of variation (247 ± 178 ppm), together with large and variable Mg# = 0.43 ± 0.34. In conclusion, the fine-grained charnockite can be considered as I-type granite. It may represent anatectic melts that have intruded into the fayalite-bearing charnockitoid before being affected by the same deformation episode (M1).

Leucocharnockite dyke

In the field, the leucocharnockite (#G7) is a foliated dyke in the fayalite-bearing charnockitoid. The rock is hololeucocratic and depleted in mafic minerals and HFSE trace elements (Figs. 7 & 8). The characteristic trait is a low REE content with a positive Eu anomaly (Fig. 9D). Since the pioneering work of Barbey et al. (1989) and Sawyer (1991), this is diagnostic of anatectic processes in disequilibrium conditions with rapid extraction from the source rocks and possible sorting of quartzofeldspathic minerals in the injection process. Similar rocks are observed in the BKSK intrusion (Duchesne & Wilmart, 1997), in leucosomes of migmatitic gneiss (Duchesne & Hertogen, 2021), and in norito-granitic septa around the Egersund–Ogna anorthosite massif (Duchesne & Grard, 2021). We suggest this dyke #G7 results from a back-veining process of such anatectic melt.

Late-stage quartz monzonite dyke

The late-stage quartz monzonite dyke #G4 has many characteristics common with the charnockitic facies of the Farsund charnockite-granite pluton (Bolle et al., 2010; Vander Auwera et al., 2014a). Except for a higher Mg#, its composition is close to sample #AD011 (Fig. 15) that is considered as the parental magma at the start of the charnockitic evolution trend of the Farsund pluton in the model developed by Vander Auwera et al. (2014a). The age of the dyke is unknown but the obliquity of the dyke to the main foliation shows that it intruded in a late stage of the magmatic evolution. Its foliation, however, points to an emplacement before the main stage of deformation (M1).

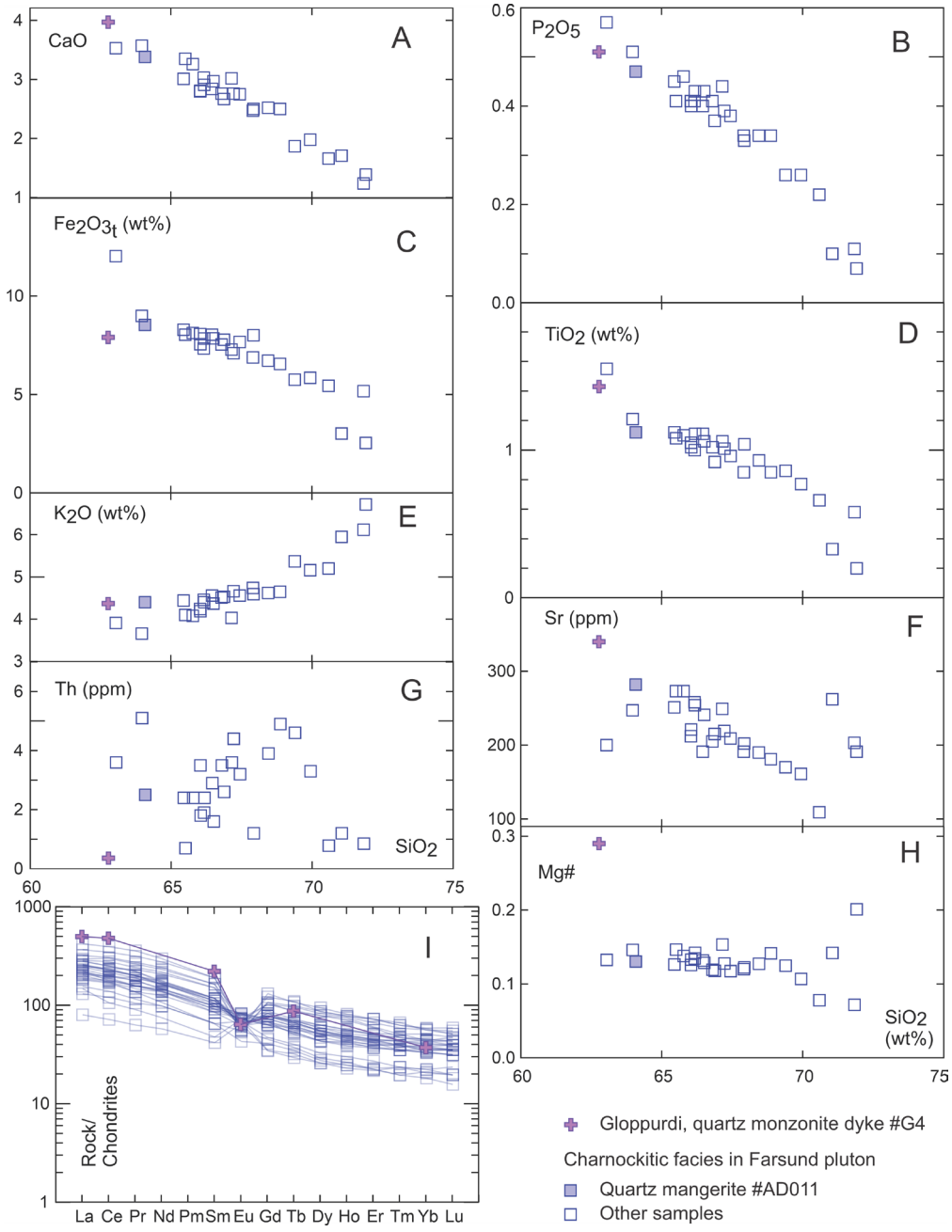

Figure 15. (A–H) Harker diagrams and (I) chondrite-normalized REE diagram comparing quartz monzonite dyke sample #G4 to the trend of the charnockitic facies in the Farsund pluton (931 ± 2 Ma; Vander Auwera et al. 2014a; Fig. 1).

Mafic rocks

As shown earlier, mafic rocks (biotite-bearing amphibolite) that are interlayered in the Gloppurdi and Botnavatn intrusions were not mafic magmas contemporaneous with the felsic magmas. Indeed, multiple lines of evidence show that they were already solid rocks when invaded by felsic magma with sharp contacts (Fig. 4B, D). This suggests that they were septa or enclaves of host gneiss in the felsic magma chamber. The geochemical composition of the mafic rocks supports this interpretation. In Fig. 16, the mafic rocks (#G10, #G17, #G8, and #B5) are compared to mafic rocks from the country gneiss complex close to the RAP (Duchesne & Hertogen, 2021). Three types of mafic rocks were defined in that work: amphibolite (without biotite), biotite-bearing amphibolite and jotunitic amphibolite. Harker diagrams for immobile elements such as Ti, P and Zr show that mafic rocks in Gloppurdi and Botnavatn plot between the biotite-bearing and jotunitic amphibolites (Fig. 16A–C). The REE distributions (Fig. 16E) confirm the similarity with the biotite-bearing amphibolite. The geochemical composition of the mafic rocks is thus consistent with the mineralogy of biotite-bearing amphibolite. In conclusion, the mafic rocks are interpreted as septa or enclaves of country rocks and do not result from the crystallization of a mafic magma coeval with the felsic magma. A bimodal association of mafic and felsic magmas is thus precluded.

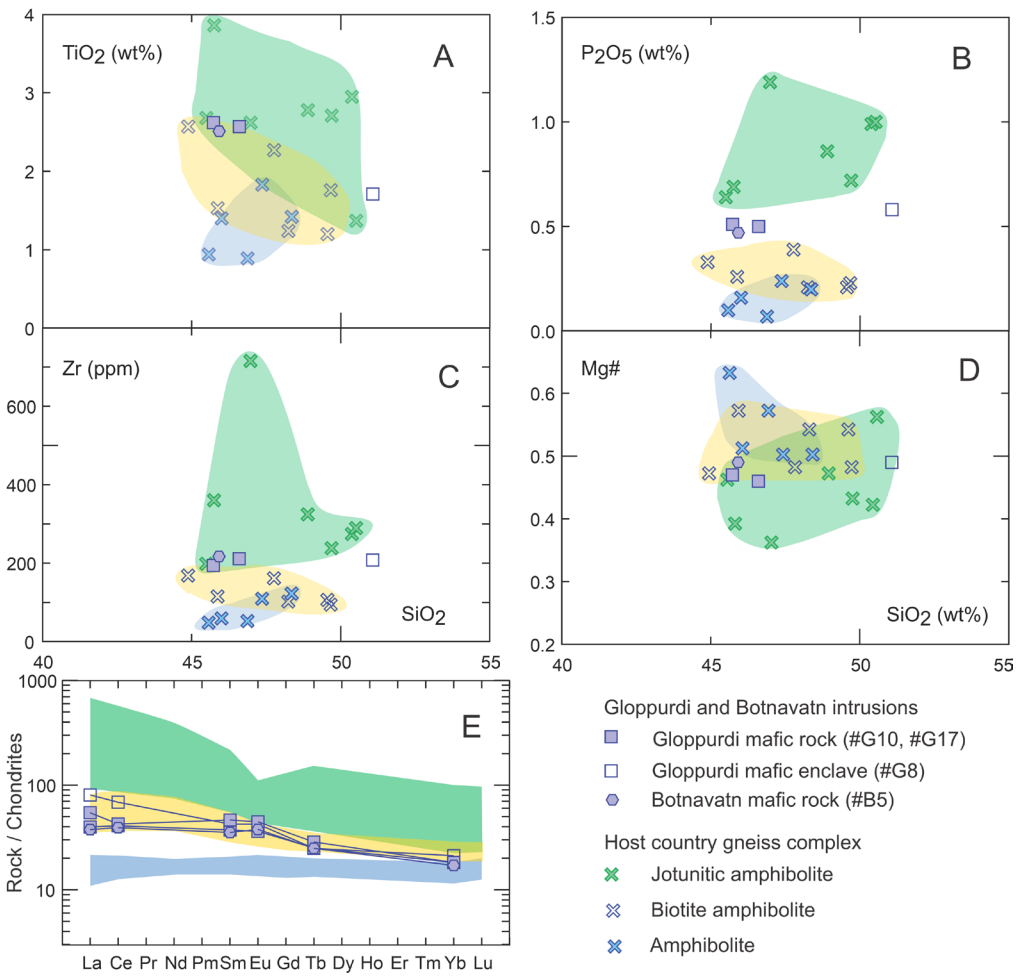

Figure 16. (A–D) Harker diagrams and (E) chondrite-normalized REE diagram comparing mafic rocks from Gloppurdi and Botnavatn to various types of amphibolite in the gneiss complex forming the wall rocks of the RAP (Duchesne & Hertogen, 2021).

Implications

Concealed anorthosite magmatic system

Fayalite-bearing charnockitoid in the Gloppurdi and Botnavatn intrusions has major elements similar to the fayalite-bearing trend of the BKSK layered intrusion (Figs. 11 & 12). It shows Zr, Th and REE compositions (Fig. 13) that relate / bind it to the Zr-rich jotunite / ferromonzodiorite in the RAP. As noted above, these Zr-rich rocks are typically related to anorthosites in a number of AMCG provinces, particularly in the RAP (Duchesne & Liégeois, 2015). The fayalite-bearing charnockitoid in the Gloppurdi and Botnavatn is therefore interpreted to represent fractionated products of the Zr-rich jotunite trend, typical of AMCG provinces. It can represent the top of a layered structure similar to the BKSK intrusion, where the fayalite-bearing trend lies above layered anorthosite and norite and is associated with large anorthosite massifs. Here we speculate that an AMCG magmatic system, itself resulting from a complex polybaric petrogenesis, was therefore present at c. 1240 Ma.

While the geochemical link is clear, the geological evidence for a concealed AMCG magmatic system is tenuous. Regional scale gravity and magnetic geophysical data do not show specific anomalies in the Gloppurdi and Botnavatnet area interpretable as evidence for a separate anorthosite complex east of the much larger RAP (Olesen et al., 2013, their line 3 in their Fig. 12.39). However, specific modelling along a NNW–SSE transect southeast of Stavanger (anchored at the Ullrigg borehole, Fig. 1) proposes a c. 3 km thick body with properties of anorthosite and norite sandwiched in felsic gneiss at a depth of c. 4 km (Olesen et al., 2013, their line 4 in their Fig. 13.14). This body could have any age between 0.93 and 1.52 Ga. This model is thus compatible with the interpretation of a concealed 1.24 Ga AMCG magmatic system.

Episodic AMCG plutonism

Geochronological data for a number of Proterozoic AMCG provinces show a significant spread of dates. This dispersion can be interpreted in terms of episodic magmatism or alternatively protracted magmatism. Episodic means that several independent AMCG magmatic systems recur at different points in time in the same area, while protracted means that individual magmatic systems are long-lived and producing a diversity of products over an extended time interval. The two lines of interpretation are not mutually exclusive. For example, in the Nain batholith (Labrador; Hamilton et al., 1998; Connely & Ryan, 1999; Myers et al., 2008; Fourny et al., 2019), the Laramie Anorthosite Complex (Wyoming; Scoates and Chamberlain, 1997), the Lac-Saint-Jean anorthosite suite (Grenville orogen, Québec; Higgins & van Breemen, 1996; Higgins, et al., 2002), the Kunene Anorthosite Complex (Namibia; Bybee et al., 2019) and the Turkel Anorthosite Complex (Eastern Ghats, India; Raith et al., 2014), AMCG plutonism is organized in up to three distinct magmatic suites, each up to 30 Myr long, typically starting each with anorthosite and closing with granite.

The most intriguing evidence for periodicity comes from Sm–Nd isochrons collected on high-alumina orthopyroxene megacrysts (HAOMs) hosted in anorthosite plutons. For three of the anorthosite provinces, HAOMs yield Sm–Nd isochron age older by c. 80 to 120 Myr than the intrusion age of their host anorthosite as defined by zircon U–Pb geochronology (Bybee et al., 2014). In the RAP, samples of HAOM with Al2O3 content higher than 8 wt.% hosted in the Egersund–Ogna anorthosite massif yield an Sm–Nd isochron at 1040 ± 17 Ma (Bybee et al., 2014). This indicates that the anorthosite plutonism began at greater depths some 110 Myr before final intrusion. These data can be interpreted as evidence for extremely long-lived magma chambers carrying antecrystic HAOMs

formed at the base of the crust (Moho depth; Bybee et al., 2014) or alternatively evidence for episodic magmatism carrying xenocrystic HAOMs inherited from a source situated at Moho depth or inherited from a previous independent magmatic event (Vander Auwera et al., 2014*b*).

In Rogaland, AMCG plutonism culminated with the emplacement of the RAP at mid-crustal level between c. 932 and 915 Ma (Schärer et al., 1996; Vander Auwera et al., 2011). Independently of their petrological interpretation, the HAOMs reveal an earlier pulse of this magmatism at 1040 ± 17 Ma (Bybee et al., 2014; Vander Auwera et al., 2014*b*). The present work leads to the interpretation of a first independent episode of AMCG plutonism at c. 1236 Ma associated with the Gloppurdi and Botnavatn intrusions. This long history had a final surge with intrusion at 855 ± 59 Ma of the Hunnedalen dyke swarm, made up of jotunite in all points similar to the BKSK and Hidra parental magmas (Maijer & Verschure, 1998). These dykes are not deformed which implies that they postdate the last regional deformation phase.

Geotectonic setting

As bluntly stated by Ashwal and Bybee (2017), *"virtually every known tectonic setting has been proposed for the generation of massif-type anorthosites".* Early studies showed that AMCG provinces occur in cratonic zones and therefore suggested that AMCG plutonism is product of mantle plumes or continental rifting (Emslie, 1978, 1985). However, these studies also pointed out that anorthosite occurs in Proterozoic orogenic zones, some of them juvenile, and that the tectonic setting of intrusion may be difficult to evaluate. This is the case for the RAP in the Sveconorwegian orogen, for which two lines of interpretation dominate. Anorthosite massifs are related to orogenic decay, meaning that they are linked to crustal extension following Sveconorwegian collision and crustal thickening (Duchesne et al., 1999; Vander Auwera et al., 2011; Bingen et al., 2021). Alternatively, they are located in a back-arc setting, behind a retreating subduction zone (Ashwal & Bybee, 2017; Slagstad et al., 2018; Granseth et al., 2020; Slagstad et al., 2022). Both these settings are extensional, are characterized by a hot Moho and provide a heat source via asthenospheric mantle upwelling.

Episodic AMCG plutonism over time intervals exceeding 100 Myr in a specific area rules out a relationship between AMCG plutonism and a single mantle plume (presumably short-lived). Instead, it suggests that AMCG plutonism can result from repeated activation of lithospheric-scale structures above a Proterozoic mantle persistently hotter than today's normal mantle (Korenaga, 2018). Detailed structural work has emphasized the role of linear delamination leading to UHT conditions in lithospheric-scale tectonic structures such as large faults (Bogdanova et al., 2004; Myers et al., 2008; Duchesne et al., 2010), terrane boundaries (Ryan, 2000) or shear zones (van Breemen & Higgins, 1993; Bolle et al., 2010). Importantly, in a number of these cases the weakness zone is much older than the anorthosite intrusion, which suggests its possible reactivation (Scoates & Chamberlain, 1995; Hamilton et al., 1998; Vander Auwera et al., 2014b). Episodic activation of large-scale weakness zones possibly activated magma sources several times and facilitated diapiric rise and ballooning of anorthosite massifs to middle crustal level.

In South Norway, east–west trending offshore deep seismic profiles, perpendicular to the Sveconorwegian structural trend are interpreted as stacking of the Sveconorwegian crust with subduction / underthrusting of the lower crust (decoupled from the upper crust) forming crustal tongues in the mantle and Moho offsets (Andersson et al., 1996). On this premise, Duchesne et al. (1999) proposed that delamination and asthenospheric upwelling along these tongues could have brought sufficient heat to melt mafic rocks in them, to produce the high-alumina basaltic melt and other parental melts and to form the deep-seated magma chambers in which anorthosite magmatism could develop. Scars of this process are still visible in the seismic profiles as major lithospheric structures

linked to Moho offsets. Recent structural studies suggest that the surface expression of a Moho offset SE of the RAP probably corresponds to the NNW–SSE trending Farsund Shear Zone defined by Bolle et al. (2010) and Vander Auwera et al. (2014*a*) (Fig. 1). This shear zone is situated along the margin and in the country rock of the RAP and is interpreted to have controlled emplacement of the anorthosite province at c. 930 Ma. Northwards, the Farsund Shear Zone links to the Rogaland Extensional Detachment (RED) defined by Slagstad et al. (2022) (Fig. 1). The Farsund Shear Zone was active for a long time, at least between 1050 and 930 Ma as revealed by incorporation of augen gneiss of the Sirdal magmatic suite in its eastern contact zone (Duchesne & Hertogen, 2021). Also, jotunitic rocks older than the c. 930 Ma (Duchesne & Hertogen, 2021) could well be related to the pulse of HAOM crystallisation at 1040 ± 17 Ma identified by Bybee et al. (2014). Intrusion of the Hunnedalen jotunitic dykes at 855 ± 59 Ma, east of the Farsund Shear Zone and east (in the hanging wall) of the Rogaland Extensional Detachment, represents a youngest limit for displacement along these shear zones.

The geotectonic setting prevailing between 1280 and 1140 Ma, i.e., the time interval that includes the intrusion of the Gloppurdi and Botnavatn intrusions (1236 ± 8 Ma), is continental, extensional and within-plate over the entire Sveconorwegian orogen (Bingen et al., 2021). In the Telemarkia lithotectonic unit, this time interval is characterized by several pulses of bimodal (mafic-felsic) magmatism (plutonism and volcanism), intrusion of voluminous ferroan A-type granite plutons and continental fault-bounded intramontane sedimentary basins (Andersen et al., 2009; Lamminen, 2011; Bingen & Viola, 2018). Considering the signature of magmatism, sedimentation and tectonic regime, Bingen & Viola (2018) argued that a first (pre-Sveconorwegian) event of subcontinental lithospheric mantle delamination took place after 1280 Ma in the Telemarkia lithotectonic unit. That would be favourable to genesis of AMCG plutonism. Interpretation of the geochemistry of the c. 1236 Ma Gloppurdi and Botnavatn intrusions is compatible with this geotectonic interpretation. It is important to note that amongst A-type granites, the Hidderskog (1159 ± 5 Ma), Gjeving (1152 ± 11 Ma), Ubergsmoen (1150 ± 13 Ma) and Hovdefjell (1140 ± 13 Ma) intrusions (in the Telemarkia and Bamble lithotectonic units; Fig. 1) are known charnockitic metaplutons (Touret, 1967; Zhou et al., 1995; Bingen & Viola, 2018). These intrusions contain foliated orthopyroxene-bearing quartz mangerite and charnockite and attest to more charnockitic plutonism in the 1280–1140 Ma time interval. However, their calc-alkaline geochemical signature (Fig. 11) suggests they are not related to any concealed AMCG complex.

The Gloppurdi and Botnavatn intrusions are located just east of the Farsund Shear Zone and the Rogaland Extensional Detachment. Here we speculate that precursors of Farsund Shear Zone and Rogaland extensional detachment were possibly activated as early as 1.24 Ga in a context of crustal extension.

Conclusions

- The Gloppurdi and Botnavatn intrusions are composite intrusions dominated by fayalite-bearing charnockitoid (mangerite, quartz mangerite and charnockite), associated with fine-grained leucocratic charnockite, leucocharnockite dykes, late-stage quartz monzonite dykes and biotite-amphibolite xenoliths. They formed at 1236 ± 8 Ma and were metamorphosed during the regional M1 event at 1013 ± 12 Ma.
- The characteristic fayalite-bearing charnockitoid is ferroan (Mg# < 0.1), alkalic and metaluminous. The large variation in composition (60 < SiO_2 < 75 wt.%) can be explained by variable clustering of mafic minerals. It has a major element composition similar to the fayalite-bearing quartz mangerite of the Bjerkreim–Sokndal (BKSK) layered intrusion. The Zr, REE, Th and U compositions link them to the Zr-rich jotunite kindred, typically found in AMCG provinces.

- The fine-grained leucocratic charnockite is interpreted as product of anatexis of country rock.

Geochemistry links the Gloppurdi and Botnavatn fayalite-bearing charnockitoid to AMCG plutonism, leading to the following suggestions and speculations:

- A concealed AMCG magmatic system was possibly present at depth at c. 1240 Ma.
- At regional scale, there is evidence for episodic AMCG plutonism, with a possible early episode at c. 1240 Ma, a main episode at 932–915 Ma with the RAP and a final episode at c. 850 Ma with the jotunitic Hunnedalen dykes.
- AMCG plutonism at c. 1240 Ma is compatible with continental, within-plate, extensional tectonic regime inferred in the 1280 and 1140 Ma time interval.
- The Farsund Shear Zone (and Rogaland Extensional Detachment) that controlled the emplacement of the RAP at c. 930 Ma were possibly active at c. 1240 Ma to channel the intrusion of the Gloppurdi and Botnavatn intrusions.

Acknowledgements. We thank Guy Bologne for help with chemical analyses. The trace elements in sample #72–145b were determined by Jan Hertogen. BB and MHH used projects # 388500 and 325100 of the Geological Survey of Norway. We acknowledge access to the MIMAC laboratory (Norwegian research council project # 269842/F50). Grant Bybee, Sebastian Tappe and Michael Higgins are thanked for constructive critical review and Espen Torgersen for editorial management.

References

Andersen, T., Graham, S. & Sylvester, A.G. 2007: Timing and tectonic significance of Sveconorwegian A-type granitic magmatism in Telemark, southern Norway: new results from Laser-abalation ICPMS U–Pb dating of zircon. *Norges geologisk undersøkelse Bulletin 447*, 17–31.

Andersen, T., Graham, S. & Sylvester, A.G. 2009: The geochemistry, Lu–Hf isotope systematics, and petrogenesis of late Mesoproterozoic A-type granites in southwestern Fennoscandia. *Canadian Mineralogist 47*, 1399–1422. https://doi.org/10.3749/canmin.47.6.1399

Andersson, M., Lie, J.E. & Husebye, E.S. 1996: Tectonic setting of post-orogenic granites within SW Fennoscandia based on deep seismic and gravity data. *Terra Nova 8*, 558–566. https://doi.org/10.1111/j.1365-3121.1996.tb00785.x

Ashwal, L.D. 1993: *Anorthosites.* Springer Berlin, Heidelberg, 422 pp. https://doi.org/10.1007/978-3-642-77440-9

Ashwal, L.D. & Bybee, G.M. 2017: Crustal evolution and the temporality of anorthosites. *Earth-Science Reviews 173*, 307–330. https://doi.org/10.1016/j.earscirev.2017.09.002

Barbey, P., Bertrand, J.M., Angoua, S. & Dautel, D. 1989: Petrology and U/Pb geochronology of the Telohat migmatites, Aleksod, Central Hoggar, Algeria. *Contributions to Mineralogy and Petrology 101*, 207–219. https://doi.org/10.1007/BF00375307

Bingen, B. & van Breemen, O. 1998: Tectonic regimes and terrane boundaries in the high-grade Sveconorwegian belt of SW Norway, inferred from U–Pb zircon geochronology and geochemical signature of augen gneiss suites. *Journal of the Geological Society of London 155,* 143–154. https://doi.org/10.1144/gsjgs.155.1.0143

Bingen, B., Skår, Ø., Marker, M., Sigmond, E., Nordgulen, Ø., Ragnhildsveit, J., Mansfeld, J., Tucker, R.D. & Liégeois, J.-P. 2005: Timing of continental building in the Sveconorwegian orogen, SW Scandinavia. *Norwegian Journal of Geology 85*, 87–116.

Bingen, B., Nordgulen, Ø. & Viola, G. 2008: A four-phase model for the Sveconorwegian orogeny. *Norwegian Journal of Geology 88,* 43–72.

Bingen, B. & Viola, G. 2018: The early-Sveconorwegian orogeny in southern Norway: tectonic model involving delamination of the sub-continental lithospheric mantle: *Precambrian Research 313*, 170–204. https://doi.org/10.1016/j.precamres.2018.05.025

Bingen, B., Viola, G., Moller, C., Vander Auwera, J., Laurent, A. & Keewook, Y. 2021: The Sveconorwegian orogeny. *Gondwana Research 90*, 273–313. https://doi.org/10.1016/j.gr.2020.10.014

Blereau, E., Johnson, T., Clark, C., Taylor, R., Kinny, P. & Hand, M. 2017: Reappraising the P–T evolution of the Rogaland–Vest Agder Sector, southwestern Norway. *Geoscience Frontiers 8*, 1–14. https://doi.org/10.1016/j.gsf.2016.07.003

Boehnke, P., Watson, E.B., Trail, D., Harrison, T. & Schmitt, A.K. 2013: Zircon saturation re-visited. *Chemical Geology 351*, 324–334. https://doi.org/10.1016/j.chemgeo.2013.05.028

Bogdanova, S., Pashkevich, I.K., Buryanov, V.B., Makarenko, I.V., Orlyuk, M.I., Skobelev, V.M., Starostenko, V.I. & Legostaeva, O.V. 2004: The 1.80-1.74 Ga anorthosite-rapakivi granite Korosten Pluton in the Ukrainian Shield: a 3-D geophysical reconstruction of deep structure. *Tectonophysics 381*, 5–27. https://doi.org/10.1016/j.tecto.2003.10.023

Bolle, O., Demaiffe, D. & Duchesne, J.C. 2003: Petrogenesis of jotunitic and acidic members of an AMC suite (Rogaland anorthosite province, SW Norway): a Sr and Nd isotopic assessment. *Precambrian Research 124,* 185–214. https://doi.org/10.1016/S0301-9268(03)00086-X

Bolle, O., Diot, H., Liégeois, J.-P. & Vander Auwera, J. 2010: The Farsund intrusion (SW Norway): A marker of late-Sveconorwegian (Grenvillian) tectonism along a newly defined major shear zone. *Journal of Structural Geology 32,* 1500–1518. https://doi.org/10.1016/j.jsg.2010.04.003

Bolle, O., Diot, H., Vander Auwera, J., Dembele, A., Schittekat, J., Spassov, S., Ovtcharova, M. & Schaltegger, U. 2018: Pluton construction and deformation in the Sveconorwegian crust of SW Norway: magnetic fabric and U–Pb geochronology of the Kleivan and Sjelset granitic complexes. *Precambrian Research 305,* 247–267. https://doi.org/10.1016/j.precamres.2017.12.012

Bolle, O. & Duchesne, J.C. 2007: The apophysis of the Bjerkreim–Sokndal layered intrusion (Rogaland anorthosite province, SW Norway): a composite pluton build up by tectonically-driven emplacement of magmas along the margin of an AMC igneous complex. *Lithos 98*, 292–312. https://doi.org/10.1016/j.lithos.2007.05.002

Boudreau, A. 1999: PELE- a version of the MELTS software program for the PC platform. *Computers & Geosciences 25,* 201–203. https://doi.org/10.1016/S0098-3004(98)00117-4

Bybee, G.M., Ashwal, L.D., Shirey, S., Horan, M., Mock, T. & Andersen, T. 2014: Pyroxene megacrysts in Proterozoic anorthosites: Implications for tectonic setting, magma source and magmatic processes at the Moho. *Earth and Planetary Science Letters 389*, 74–85. https://doi.org/10.1016/j.epsl.2013.12.015

Bybee, G.M., Hayes, B., Owen-Smith, T.M., Lehmann, J., Ashwal, L.D., Brower, A.M., Hill, C.M., Corfu, F. & Manga, M. 2019: Proterozoic massif-type anorthosites as the achetypes of long-lived (>100 Myr) magmatic systems - New evidence from the Kunene Anorthosite Complex (Angola). *Precambrian Research 332*, 105393. https://doi.org/10.1016/j.precamres.2019.105393

Chappell, B.W. 1999: Aluminium saturation in I- and S-type granites and the characterization of fractionated haplogranites. *Lithos 46,* 535–551. https://doi.org/10.1016/S0024-4937(98)00086-3

Charlier, B., Vander Auwera, J. & Duchesne, J.C. 2005: Geochemistry of cumulates from the Bjerkreim–Sokndal layered intrusion (S. Norway). Part II: REE and the trapped liquid fraction. *Lithos 83,* 255–276. https://doi.org/10.1016/j.lithos.2005.03.005

Charlier, B., Duchesne, J.C., Vander Auwera, J., Storme, J.-Y., Maquil, R. & Longhi, J. 2010: Polybaric fractional crystallization of high-alumina basalt parental magmas in the Egersund–Ogna massif-type anorthosite (Rogaland, SW Norway) constrained by plagioclase and high-alumina orthopyroxene megacrysts. *Journal of Petrology 51*, 2547–2570. https://doi.org/10.1093/petrology/egq066

Coint, N., Slagstad, T., Roberts, N.M.W., Marker, M., Røhr, T.S. & Sørensen, B.E. 2015: The Late Mesoproterozoic Sirdal Magmatic Belt, SW Norway: relationships between magmatism and metamorphism and implications for Sveconorwegian orogenesis. *Precambrian Research 265*, 57–77. https://doi.org/10.1016/j.precamres.2015.05.002

Connelly, J.N. & Ryan, B. 1999: Age and tectoic implications of Paleoproterozoic granitoids intrusions within the Nain Province near Nain, Labrador. *Canadian Journal of Earth Sciences 36,* 833–853. https://doi.org/10.1139/e99-002

Demaiffe, D. & Hertogen, J. 1981: Rare earth element geochemistry and strontium isotopic composition of a massif-type anorthositic-charnockitic body: the Hidra massif (Rogaland, SW. Norway). *Geochimica et Cosmochimica Acta 45*, 1545–1561. https://doi.org/10.1016/0016-7037(81)90284-2

Drüppel, K., Elsäber, L., Brandt, S. & Gerdes, A. 2013: Sveconorwegian mid-crustal ultrahigh-temperature metamorphism in Rogaland, Norway: U–Pb LA–ICP–MS geochronology and pseudosections of sapphirine granulites and associated paragneisses. *Journal of Petrology 54*, 305–350. https://doi.org/10.1093/petrology/egs070

Duchesne, J.C. & Charlier, B. 2005: Geochemistry of cumulates from the Bjerkreim–Sokndal layered intrusion (S. Norway). Part I: Constraints from major elements on the mechanism of cumulate formation and on the jotunite liquid line of descent. *Lithos 83,* 229–254. https://doi.org/10.1016/j.lithos.2005.03.004

Duchesne, J.C. & Grard, A. 2021: Evidence of crustal disequilibrium melting, mingling processes, layering and deformation in UHT conditions: the marginal zone of the Egersund-Ogna massif-type anorthosite (S. Norway). *Lithos 398–399*, 106267. https://doi.org/10.1016/j.lithos.2021.106267

Duchesne, J.C. & Hertogen, J. 1988: Le magma parental du lopolithe de Bjerkreim–Sokndal (Norvège méridionale). *Comptes Rendus de l'Académie des Sciences de Paris 306*, 45–48.

Duchesne, J.C. & Hertogen, J. 2021: The Farsund Shear Zone: geochemical evidence for lithological diversity in the wall rock of the Rogaland Anorthosite Province, South Norway. *Norwegian Journal of Geology 100*, 1–23. https://doi.org/10.17850/njg100-4-3

Duchesne, J.C. & Liégeois, J.-P. 2015: The origin of nelsonite and high-Zr ferrodiorite associated with Proterozoic anorthosite. *Ore Geology Review 71*, 40–56. https://doi.org/10.1016/j.oregeorev.2015.05.005

Duchesne, J.C. & Wilmart, E. 1997: Igneous charnockites and related rocks from the Bjerkreim–Sokndal layered intrusion (Southwest Norway): a jotunite (hypersthene monzodiorite)-derived A-type granitoid suite. *Journal of Petrology 38*, 337–369. https://doi.org/10.1093/petroj/38.3.337

Duchesne, J.C., Demaiffe, D., Roelandts, I. & Weis, D. 1985a: Petrogenesis of monzonoritic dykes in the Egersund–Ogna anorthosite (Rogaland, S.W. Norway): trace elements and isotopic constraints. *Contribution to Mineralogy and Petrology 90,* 214–225. https://doi.org/10.1007/BF00378262

Duchesne, J.C., Maquil, R. & Demaiffe, D. 1985*b*: The Rogaland anorthosites: facts and speculations. *In* Tobi, A.C. & Touret, J.L.R. (eds.): *The deep Proterozoic crust in the North Atlantic Province,* NATO–ASI C158, Reidel, Doordrecht, pp. 449–476. https://doi.org/10.1007/978-94-009-5450-2_27

Duchesne, J.C., Liégeois, J.P., Vander Auwera, J. & Longhi, J. 1999: The crustal tongue melting model and the origin of massive anorthosites. *Terra Nova 11,* 100–105. https://doi.org/10.1046/j.1365-3121.1999.00232.x

Duchesne, J.C., Vander Auwera, J., Liégeois, J.-P., Barton, E. & Clifford, T. 2007: Geochemical contraints on the petrogenesis of the O'okiep Koperberg Suite and Granitic plutons (Namaqualand, S. Africa): a lower crustal mafic source in Namaquan (Grenville) times. *Precambrian Research 153*, 116–142. https://doi.org/10.1016/j.precamres.2006.11.005

Duchesne, J.C., Martin, H., Baginski, B., Wiszniewska, J. & Vander Auwera, J. 2010: The origin of ferroan-potassic A-type granitoids: the case of the hornblende-biotite granite suite of the Mesoproterozoic Mazury Complex, northeastern Poland. *Canadian Mineralogist 48*, 1195–1216. https://doi.org/10.3749/canmin.48.4.947

Emslie, R. 1975: Pyroxene megacrysts from anorthositic rocks: new clues to the sources and evolution of the parent magmas. *Canadian Mineralogist 13*, 138–145.

Emslie, R.F. 1978: Anorthosite massifs, Rapakivi granites, and the late Proterozoic rifting of North America. *Precambrian Research 7*, 61–98. https://doi.org/10.1016/0301-9268(78)90005-0

Emslie, R.F. 1985: Proterozoic anorthosite massifs. *In* Tobi, A.C. & Touret, J.L.R. (eds.): *The deep Proterozoic crust in the North Atlantic Provinces*, NATO–ASI C158, Reidel, Dordrecht, pp. 39–60. https://doi.org/10.1007/978-94-009-5450-2_4

Emslie, R.F., Hamilton, M.A. & Thiérault, R.J. 1994: Petrogenesis of a Mid-Proterozoic Anorthosite - Mangerite - Charnockite - Granite (AMCG) complex: isotopic and chemical evidence from the Nain plutonic suite. *Journal of Geology 102*, 539–558. https://doi.org/10.1086/629697

Falkum, T., 1982: Geologisk kart over Norge, berggrunnskart Mandal, scale 1:250,000, *Norges Geologiske Undersøkelse.*

Fourny, A., Weis, D. & Scoates, J.S. 2019: Isotopic and trace element geochemistry of the Kiglapait intrusion, Labrador: deciphering the mantle source, crustal contributions and processes preserved in mafic layered intrusions. *Journal of Petrology 60,* 553–590. https://doi.org/10.1093/petrology/egz006

Frost, B.R., Barnes, C.G., Collins, W.J., Arculus, R.J., Ellis, D.J. & Frost, C.D. 2001: A geochemical classification for granitic rocks. *Journal of Petrology 42*, 2033–2048. https://doi.org/10.1093/petrology/42.11.2033

Granseth, A., Slagstad, T., Coint, N., Roberts, N.M.W., Røhr, T.S. & Sørensen, B.E. 2020: Tectono-magmatic evolution of the Sveconorwegian orogen recorded in the chemical and isotopic compositions of 1070–920 Ma granitoids. *Precambrian Research 340,* 105527. https://doi.org/10.1016/j.gr.2020.10.019

Hamilton, M.A., Ryan, A.B., Emslie, R.F. & Ermanovics, I.F. 1998: Identification of Paleaoproterozoic anorthosititic and monzonitic rocks in the vicinity of the Mesoproterozoic Nain Plutonic Suite, Labrador: U–Pb evidence. *Geological Survey of Canada, Current Research 1998–F,* 23–40. https://doi.org/10.4095/210053

Harley, S.L. 2008: Refining the P–T records of UHT crustal metamorphism. *Journal of Metamorphic Geology 26*, 125–154. https://doi.org/10.1111/j.1525-1314.2008.00765.x

Harrison, T.M. & Watson, E.B. 1984: The behavior of apatite during crustal anatexis: equilibrium and kinetic considerations. *Geochimica Cosmochimica Acta 48*, 1467–1477. https://doi.org/10.1016/0016-7037(84)90403-4

Hermans, G.A.E.M., Tobi, A.C., Poorter, R.P.E. & Maijer, C. 1975: The high-grade metamorphic Precambrian of the Sirdal–Ørsdal area, Rogaland / Vest–Agder, SW Norway. *Norges geologiske undersøkelse 318*, 51–74.

Higgins, M.D. & van Breemen, O. 1996: Three generations of anorthosite-mangerite-charnockite-granite (AMCG) magmatism, contact metamorphism and tectonism in the Saguenay-Lac-Saint-Jean region of the Grenville Province, Canada. *Precambrian Research 79*, 327–346. https://doi.org/10.1016/0301-9268(95)00102-6

Higgins, M.D., Mohcine, I. & van Breemen, O. 2002: U–Pb ages plutonism, wollastonite formation, and deformation in the central part of the Lac-Saint-Jean anorthosite suite. *Canadian Journal of Earth Sciences 39*, 1093–1105. https://doi.org/10.1139/e02-033

Jackson, S.E., Pearson, N.J., Griffin, W.L. & Belousova, E.A. 2004: The application of laser ablation inductively coupled plasma-mass spectrometry to in situ U–Pb zircon geochronology. *Chemical Geology 211*, 47–67. https://doi.org/10.1016/j.chemgeo.2004.06.017

Jaffrezic, H., Joron, J.-L., Treuil, M. & Wood, D.A. 1980: A study of the precision attained by neutron activation analysis using international rocks GSN and BCR1 as examples. J*ournal of Radioanalytical Analysis 55*, 417–425. https://doi.org/10.1007/bf02514425

Kars, H., Jansen, J.B.H., Tobi, A.C. & Poorter, R.P.E. 1980: The metapelitic rocks of the poly-metamorphic Precambrian of Rogaland, SW Norway. Part II. Mineral relations between cordierite, hercynite and magnetite within the osumilite isograd. *Contributions to Mineralogy and Petrology 74*, 235–244. https://doi.org/10.1007/BF00371693

Korenaga, J. 2018: Crustal evolution and mantle dynamics through Earth history. *Philosophical Transactions of the Royal Society A: Mathematical, Physical and Engineering Sciences 376,* 20170408. https://doi.org/10.1098/rsta.2017.0408

Krause, O., Dobmeier, C., Raith, M. & Mezger, K. 2001: Age of emplacement of massif-type anorthosites in the Eastern Ghats Belt, India: constraints from U–Pb zircon dating and structural studies. *Precambrian Research 109*, 25–38. https://doi.org/10.1016/S0301-9268(01)00140-1

Lamminen, J. & Køykkä, J. 2010: The provenance and evolution of the Rjukan Rift Basin, Telemark, south Norway: The shift from a rift basin to an epicontinental sea along a Mesoproterozoic supercontinent. *Precambrian Research 181,* 129–149. https://doi.org/10.1016/j.precamres.2010.05.017

Laurent, A.T., Bingen, B., Duchene, S., Whitehouse, M.J., Seydoux-Guillaume, A.-M. & Bosse, V. 2018*a*: Decoding a protracted zircon geochronological record in ultrahigh temperature granulite, and persistence of partial melting in the crust, Rogaland, Norway. *Contributions to Mineralogy and Petrology 173*. https://doi.org/10.1007/s00410-018-1455-4

Laurent, A.T., Duchene, S., Bingen, B., Bosse, V. & Seydoux-Guillaume, A.-M. 2018b: Two successive phases of ultrahigh temperature metamorphism in Rogaland, S. Norway: Evidence from Y-in-monazite thermometry. *Journal of Metamorphic Geology 36,* 1009–1037. https://doi.org/10.1111/jmg.12425

Le Bas, M.J., Le Maître, R.W., Streckeisen, A. & Zanettin, B. 1986: A chemical classification of volcanic rocks based on the total alkali silica diagram. *Journal of Petrology 27,* 745–750. https://doi.org/10.1093/petrology/27.3.745

Longhi, J., Vander Auwera, J., Fram, M. & Duchesne, J.C. 1999: Some phase equilibrium constraints on the origin of Proterozoic (Massif) anorthosites and related rocks. *Journal of Petrology 40*, 339–362. https://doi.org/10.1093/petroj/40.2.339

Maijer, C., Hermans, G., Tobi, A. & Jansen, J. 1987: Day 8- The metamorphuc envelope of the Rogaland intrusive complex. *In* Maijer, C. & Padget, P. (eds.): *The geology of southermost Norway, an excursion guide,* Norges geologiske undersøkelse, pp. 81–87.

Maijer, C. & Verschure, R. 1998: Petrology and isotope geology of the Hunnedalen monzonoritic dyke swarm, SW Norway: a possible late expression of Egersund Anorthosite magmatism. *Norges geologisk undersøkelse Bulletin 434*, 83–107.

Marker, M., Schiellerup, H., Meyer, G.B., Robins, B. & Bolle, O. 2003: Geological map of the Rogaland Anorthosite Province, Scale 1:75,000. *In* Duchesne, J.C. & Korneliussen, A. (eds.): *Ilmenite deposits and their geological environments*, Norges geologiske undersøkelse Special Publication 9, pp. 109–116.

McLelland, J., Bickford, M., Hill, B.M., Clechenko, C.C., Valley, J.W. & Hamilton, M.A. 2004: Direct dating of Adirondack massif anorthosite by U–Pb SHRIMP analysis of igneous zircon: implications for AMCG complexes. *Geological Society of America Bulletin 2004*, 1299–1317. https://doi.org/10.1130/B25482.1

McLelland, J., Selleck, B., Hamilton, M.A. & Bickford, M. 2010: Late- to post-tectonic setting of some major Proterozoic anorthosite - mangerite - charnockite - granite (AMCG) suites. *Canadian Mineralogist 48*, 729–750. https://doi.org/10.3749/canmin.48.4.729

Mitchell, J.N., Scoates, J.S., Frost, C.D. & Kolker, A. 1996: The geochemical evolution of anorthosite residual magmas in the Laramie Anorthosite Complex, Wyoming. *Journal of Petrology 37*, 637–660. https://doi.org/10.1093/petrology/37.3.637

Moller, C. & Andersson, J. 2018: Metamorphic zoning and behaviour of an underthrusting continental plate. *Journal of Metamorphic Geology 36*, 567–589. https://doi.org/10.1111/jmg.12304

Müller, A., Romer, R. & Pedersen, R. 2017: The Sveconorwegian Pegmatite Province – thousands of pegmatites without parental granite. *Canadian Mineralogist 55*, 283–315. https://doi.org/10.3749/canmin.1600075

Myers, J., Voordouw, R. & Tettelaar, T. 2008: Proterozoic anorthosite-granite Nain batholith: structure and instrusion processes in an active lithosphere-scale fault zone, northern Labrador. *Canadian Journal of Earth Sciences 45*, 909–934. https://doi.org/10.1139/e08-041

Nielsen, F.M., Campbell, I.H., McCulloch, M. & Wilson, J.R. 1996: A strontium isotopic investigation of the Bjerkreim–Sokndal layered intrusion, southwest Norway. *Journal of Petrology 37*, 171–193. https://doi.org/10.1093/petrology/37.1.171

Olesen, O., Bronner, M., Ebbing, J., Elvebakk, H., Gellein, J., Koziel, J., Lauritsen, T., Lutro, O., Maystrenko, Y., Müller, C., Nasuti, A., Osmundsen, P. T., Slagstad, T. & Storrø, G. 2013: Coop Phase I - Crustal Onshore-Offshore Project: *Norges Geologiske Undersøkelse report 2013.002*, 259 pp.

Paton, C., Hellstrom, J., Paul, B., Woodhead, J. & Hergt, J. 2011: Ijolite: Freeware for the visualisation and processing of mass spectrometric data. *Journal of Analytical Atomic Spectrometry.* https://doi.org/10.1039/c1ja10172b

Peccerillo, R. & Taylor, S.R. 1976: Geochemistry of Eocene calc-alkaline volcanic rocks from the Kastamonu area, northern Turkey. *Contributions to Mineralogy and Petrology 58*, 489–502. https://doi.org/10.1007/BF00384745

Petrus, J.A. & Kamber, B.S. 2012: VizualAge: A novel approach to laser ablation ICP–MS U–Pb geochronology data reduction. *Geostandards and Geoanalytical Reseach 36*, 247–270. https://doi.org/10.1111/j.1751-908X.2012.00158.x

Raith, M., Mahapatro, S., Upadhyay, D., Berndt, J., Mezger, K. & Nanda, J. 2014: Age and P–T evolution of the Neoproterozoic Turkel Anorthosite Complex, Eastern Ghats Province, India. *Precambrian Research 254,* 87–113. https://doi.org/10.1016/j.precamres.2014.08.003

Rietmeijer, F.J.M. 1979: Pyroxenes from iron-rich igneous rocks in Rogaland, SW Norway. *Geologica Ultrajectina 21*, 341 pp.

Roberts, N.M.W., Slagstad, T., Parrish, R., Norry, M.J., Marker, M. & Horstwood, M. 2013: Sedimentary recycling in arc magmas: geochemical and U–Pb–Hf–O constraints on the Mesoproterozoic Suldal Arc, SW Norway. *Contributions to Mineralogy and Petrology 165*, 507–523. https://doi.org/10.1007/s00410-012-0820-y

Robins, B., Tumyr, O., Tysseland, M. & Garmann, L.B. 1997: The Bjerkreim–Sokndal Layered Intrusion, Rogaland, S.W. Norway: Evidence from marginal rocks for a jotunite parent magma. *Lithos 39,* 121–133. https://doi.org/10.1016/S0024-4937(96)00021-7

Roelandts, I. & Duchesne, J.C. 1979: Rare-earth elements in apatite from layered norites and iron-titanium oxide ore-bodies related to anorthosites (Rogaland, S.W. Norway). *In* Ahrens, L.H. (ed.): *Origin and distribution of the elements,* Pergamon, pp. 199–212. https://doi.org/10.1016/0079-1946(79)90022-3

Ryan, B. 2000: The Nain–Churchill boundary and the Nain Plutonic Suite: A regional perspective on the geologic setting of the Voisey's Bay Ni–Cu–Co deposit. *Economic Geology 95*, 703–724. https://doi.org/10.2113/gsecongeo.95.4.703

Sawyer, E.W. 1991: Disequilibrium melting and the rate of melt-residuum separation during migmatization of mafic rocks from the Grenville Front, Quebec. *Journal of Petrology 32*, 701–738. https://doi.org/10.1093/petrology/32.4.701

Schärer, U., Wilmart, E. & Duchesne, J.C. 1996: The short duration and anorogenic character of anorthosite magmatism: U–Pb dating of the Rogaland complex, Norway. E*arth and Planetary Sience Letters 139,* 335–350. https://doi.org/10.1016/0012-821X(96)00033-7

Schiellerup, H., Lambert, D.D., Prestvik, T., Robins, B., McBride, J.S. & Larsen, R.B. 2000: Re–Os isotopic evidence for a lower crustal origin of massif-type anorthosites. *Nature 405,* 781–784. https://doi.org/10.1038/35015546

Scoates, J.S. & Chamberlain, K.R. 1995: Baddeleyite (ZrO2) and zircon (ZrSiO4) form anorthositic rocks of the Laramie anorthosite complex, Wyoming: Petrologic consequences and U–Pb ages. *American Mineralogist 80*, 1317–1327. https://doi.org/10.2138/am-1995-11-1222

Scoates, J.S. & Chamberlain, K.R. 1997: Orogenic to post-orogenic origin for the 1.76 Ga Horse Creek anorthosite complex, Wyoming, USA. *Journal of Geology 105*, 331–343. https://doi.org/10.1086/515928

Scoates, J.S. & Chamberlain, K.R. 2003: Geochronology, geochemical and isotopic constraints on the origin of monzonitic and related rocks in the Laramie anorthosite complex, Wyoming, USA. *Precambrian Research 124*, 269–304. https://doi.org/10.1016/S0301-9268(03)00089-5

Seifert, K.E., Dymek, R., Whitney, P. & Haskin, L. 2010: Geochemistry of massif anorthosite and associated rocks, Adirondack Mountains, New York. *Geosphere 6*, 855–899, https://doi.org/810.1130/GES00550.00551

Shumlyanskyy, L., Ellam, R.M. & Mitrokhin, O. 2006: The origin of basic rocks of the Korosten AMCG complex, Ukrainian shield: Implication of Nd and Sr isotope data. *Lithos 90*, 214–222. https://doi.org/10.1016/j.lithos.2006.03.004

Slagstad, T., Roberts, N.M.W., Marker, M., Røhr, T.S. & Schiellerup, H. 2013: A non collisional, accretionary Sveconorwegian orogen. *Terra Nova 25,* 30–37. https://doi.org/10.1111/ter.12001

Slagstad, T., Roberts, N.M.W., Coint, N., Høy, I., Sauer, S., Kirkland, C.L., Marker, M., Røhr, T.S., Henderson, I.H.C., Stormoen, M.A., Skår, Ø., Sørensen, B.E. & Bybee, G.M. 2018: Magma-driven, high-grade metamorphism in the Sveconorwegian Province, southwest Norway, during the terminal stages of Fennoscandian Shield evolution. *Geosphere 14*, 861–882. https://doi.org/10.1130/GES01565.1

Slagstad, T., Marker, M., Roberts, N.M.W., Saalmann, K., Kirkland, C.L., Kulakov, E., Ganerød, M., Røhr, T.S., Møkkelgierd, S.H.H., Granseth, A. & Sørrensen, B.E. 2020: The Sveconorwegian orogeny - Reamalgamation of the fragmented southwestern margin of Fennoscandia. *Precambrian Research 350,* 105877. https://doi.org/10.1016/j.precamres.2020.105877

Slagstad, T., Henderson, I.H.C., Roberts, N.M.W., Kulakov, E.V., Garnerød, M., Kirkland, C.L., Dalslåen, B., Creaser, R.A. & Coint, N. 2022: Anorthosite formation and emplacement couples with differential tectonic exhumation of ultra-high temperature rocks in a Sveconorwegian continental back-arc setting. *Precambrian Research 376,* 106695. https://doi.org/10.1016/j.precamres.2022.106695

Sláma, J., Košler, J., Condon, D. J., Crowley, J. L., Gerdes, A., Hanchar, J. M., Horstwood, M. S. A., Morris, G. A., Nasdala, L., Norberg, N., Schaltegger, U., Schoene, B., Tubrett, M. N. & Whitehouse, M. J. 2008: Plešovice zircon - A new natural reference material for U–Pb and Hf isotopic microanalysis. *Chemical Geology 249*, 1–35. https://doi.org/10.1016/j.chemgeo.2007.11.005

Streckeisen, A. 1973: Plutonic rocks: classification and nomenclature recommended by the IUGS Subcommission on the Systematics of Igneous Rocks. *Geotimes 18*, 26–30.

Streckeisen, A. 1974: How should charnockitic rocks be named? *In* Bellière, J. & Duchesne, J.C. (eds.): *Géologie des domaines cristallins*, Société Géologique de Belgique, Centenary volume, Liège, pp. 349–360.

Streckeisen, A. 1976: To each plutonic rock its proper name. *Earth-Science Reviews 12*, 1–33. https://doi.org/10.1016/0012-8252(76)90052-0

Sun, S.S. & McDonough, W.F. 1989: Chemical and isotopic systematices of oceanic basalts: implications for mantle composition and processes. *In* Saunders, A.D. & Norry, M.J. (eds.): *Magmatism in Ocean Basins*, Geological Society of London Special Publication, pp. 313–345. https://doi.org/10.1144/GSL.SP.1989.042.01.19

Tobi, A.C., Hermans, G.A.E.M., Maijer, C. & Jansen, J.B.H. 1985: Metamorphic zoning in the high - grade Proterozoic of Rogaland–Vest Agder, SW Norway. *In* Tobi, A.C. & Touret, J.L.R. (eds.): *The deep Proterozoic crust in the North Atlantic Provinces,* NATO–ASI C158, Reidel, Dordrecht, pp. 477–497. https://doi.org/10.1007/978-94-009-5450-2_28

Tomkins, H.S., Williams, I. & Ellis, D. 2005: In situ U–Pb dating of zircon formed from retrograde garnet breakdown during decompression in Rogaland, SW Norway. *Journal of Metamorphic Geology 23*, 201–215. https://doi.org/10.1111/j.1525-1314.2005.00572.x

Touret, J.L.R. 1967: Les gneiss oeillés de la région de Vegårshei–Gjerstad (Norvège méridionale). *Norwegian Journal of Geology 47*, 131–148.

van Breemen, O. & Higgins, M.D. 1993: U–Pb zircon age of the southwest lobe of the Havre-Saint-Pierre anorthosite complex, Grenville Province, Canada. *Canadian Journal of Earth Sciences 30*, 1453–1457. https://doi.org/10.1139/e93-125

Vander Auwera, J. & Longhi, J. 1994: Experimental study of a jotunite (hypersthene monzodiorite): constraints on the parent magma composition and crystallization conditions (P, T, fO2) of the Bjerkreim–Sokndal layered intrusion. *Contributions to Mineralogy and Petrology 118*, 60–78. https://doi.org/10.1007/BF00310611

Vander Auwera, J., Longhi, J. & Duchesne, J.C. 1998: A liquid line of descent of the jotunite (hypersthene monzodiorite) suite. *Journal of Petrology 39*, 439–468. https://doi.org/10.1093/petroj/39.3.439

Vander Auwera, J., Bogaerts, M., Liégeois, J.P., Demaiffe, D., Wilmart, E., Bolle, O. & Duchesne, J.C. 2003: Derivation of the 1.0–0.9 Ga ferro-potassic A-type granitoids of southern Norway by extreme differentiation from basic magmas. *Precambrian Research 124*, 107–148. https://doi.org/10.1016/S0301-9268(03)00084-6

Vander Auwera, J., Bolle, O., Bingen, B., Liégeois, J.-P., Bogaerts, M., Duchesne, J.C., De Waele, B. & Longhi, J. 2011: Sveconorwegian massif-type anorthosites and related granitoids result from post-collisional melting of a continental arc root. *Earth-Science Reviews 107*, 375–397. https://doi.org/10.1016/j.earscirev.2011.04.005

Vander Auwera, J., Bolle, O., Dupont, A., Pin, C., Paquette, J.-L., Charlier, B., Duchesne, J.C., Mattielli, N. & Bogaerts, M. 2014a: Source-derived heterogeneities in the composite (charnockite-granite) ferroan Farsund intrusion (SW Norway). *Precambrian Research 251*, 141–163. https://doi.org/10.1016/j.precamres.2014.06.003

Vander Auwera, J., Charlier, B., Duchesne, J.C., Bingen, B., Longhi, J. & Bolle, O. 2014b: Comment on Bybee et al. (2014): Pyroxene megacrysts in Proterozoic anorthosites: Implications for tectonic setting, magma source and magmatic processes at the Moho. *Earth and Planetary Science Letters 401*, 378–380. https://doi.org/10.1016/j.epsl.2014.06.031

Versteeve, A.J. 1975: Isotope geochronology in the high-grade metamorphic Precambrian of southwestern Norway. *Norges geologiske Undersøkelse 318*, 1–50.

Walderhaug, H.J., Torsvik, T.H., Eide, E.A., Sundvoll, B. & Bingen, B. 1999: Geochronology and palaeomagnetism of the Hunnedalen dykes, SW Norway: implications for the Sveconorwegian apparent polar wander loop. *Earth and Planetary Science Letters 169*, 71–83. https://doi.org/10.1016/S0012-821X(99)00066-7

Wang, C.Y., Wiest, J., Jacobs, J., Bingen, B., Whitehouse, M., Elburg, M.A., Sørstrand, T., Mikkelsen, L. & Hestnes, Å. 2021: Tracing the Sveconorwegian orogen into the Caledonides of West Norway: Geochronological and isotopic studies on magmatism and migmatization. *Precambrian Research 362*, 106301. https://doi.org/10.1016/j.precamres.2021.106301

Whalen, J.B., Currie, K.L. & Chappell, B.W. 1987: A-type granites: geochemical characteristics, discrimination and petrogenesis. *Contributions to Mineralogy and Petrology 95*, 407–419. https://doi.org/10.1007/BF00402202

Wiedenbeck, M., Allé, P., Corfu, F., Griffin, W. L., Meier, M., Oberli, F., Von Quadt, A., Roddick, J. C. & Spiegel, W. 1995: Three natural zircon standards for U–Th–Pb, Lu–Hf, trace element and REE analyses. *Geostandards Newsletter 19*, 1–23. https://doi.org/10.1111/j.1751-908X.1995.tb00147.x

Wielens, J.B.W., Andriessen, P.A.M., Boelrijk, N.A.I.M., Hebeda, E.H., Priem, H.N.A., Verdurmen, E.A.T. & Verschure, R.H. 1980: Isotope geochronology in the high-grade metamorphic Precambrian of South-western Norway: new data and reinterpretations. *Norges geologiske Undersøkelse 359*, 1–30.

Wilson, J.R., Robins, B., Nielsen, F., Duchesne, J.C. & Vander Auwera, J. 1996: The Bjerkreim–Sokndal layered intrusion, Southwest Norway. *In* Cawthorn, R.G. (ed.): *Layered Intrusions,* Elsevier, Amsterdam, pp. 231–256. https://doi.org/10.1016/S0167-2894(96)80009-1

Wiszniewska, J., Claesson, S., Stein, H.J., Vander Auwera, J. & Duchesne, J.C. 2002: The north-eastern Polish anorthosite massifs: petrological, geochemical and isotopic evidence for a crustal derivation. *Terra Nova 14*, 451–460. https://doi.org/10.1046/j.1365-3121.2002.00443.x

Zhou, X.Q., Bingen, B., Demaiffe, D., Hertogen, J., Liégeois, J.P. & Weis, D. 1995: The 1160 Ma old Hidderskog meta-charnockite: implications of this A-type pluton for the Sveconorwegian belt in Vest Agder (S.W. Norway). *Lithos 36,* 51–66. https://doi.org/10.1016/0024-4937(95)00005-Z